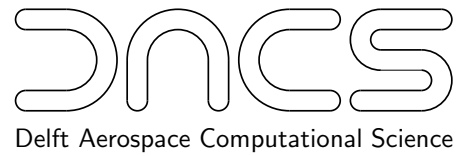




ENGINEERING MECHANICS



Delft Aerospace Computational Science

Interface-GMRES(R) Acceleration of Subiteration for Fluid-Structure-Interaction Problems

E.H. van Brummelen, C. Michler and R. de Borst

`E.H.vanBrummelen@lr.tudelft.nl`

Report DACS-05-001

January 2005

Copyright © 2005: The copyright of this manuscript resides with the author.
All rights reserved. This work may not be translated or copied
in whole or in part without the written permission of the author.

TUD/LR/EM
Kluyverweg 1, 2629HS Delft, The Netherlands
P.O. Box 5058, 2600 GB Delft, The Netherlands
Phone: +31 15 278 5460 Fax: +31 15 261 1465

ISSN 1574-6992

Interface-GMRES(R) Acceleration of Subiteration for Fluid-Structure-Interaction Problems

E.H. van Brummelen, C. Michler and R. de Borst

Delft University of Technology, Faculty of Aerospace Engineering

P.O. Box 5058, 2600 GB Delft, The Netherlands

ABSTRACT

Subiteration forms the basic iterative method for solving the aggregated equations in fluid-structure-interaction problems, in which the fluid and structure equations are solved alternately subject to complementary partitions of the interface conditions. However, this subiteration process can be defective or inadequate, as it is endowed with only conditional stability and, moreover, divergence can occur despite formal stability due to nonnormality. Furthermore, the subiteration method generally operates within a sequential time-integration process to solve a sequence of similar problems, but is unable to exploit this property. To overcome these shortcomings, the present work proposes to accelerate the subiteration method by means of a Krylov method, viz., GMRES. We show that the Krylov space can be composed of vectors in a low-dimensional subspace associated with the discrete representation of a function on the fluid-structure interface. The corresponding Interface-GMRES-acceleration procedure requires negligible computational resources, and retains the modularity of the underlying subiteration method. Moreover, the Krylov space can be optionally reused in subsequent invocations of the GMRES method, conforming to the GMRESR procedure. Detailed numerical results for a prototypical model problem are presented to illustrate the effectiveness of the proposed Interface-GMRES(R)-acceleration of the subiteration method.

2000 Mathematics Subject Classification: primary: 65N12. secondary: 35R35,

Keywords and Phrases: fluid-structure interaction, subiteration, GMRES, GMRESR, monolithic methods, convergence and stability.

1. Introduction

Numerical solution methods for fluid-structure-interaction problems are of great importance in many physical and engineering disciplines such as aerospace engineering [9, 10], civil engineering [24], offshore engineering [5] and bio-mechanics [2, 14]. Such solution methods engage two essential problems. Firstly, the profound disparity of the initial-boundary-value problems associated with the fluid and the structure generally yields severely ill-conditioned systems of equations. Secondly, the free-boundary character of the interface between the fluid and the structure yields an interdependence between the fluid and structure solutions and their domains of definition, and the computational expenses incurred by implicit treatment of this interdependence are prohibitive in actual applications. In addition, several practical impediments emanate from the inherent interconnection between the fluid and structure, such as the loss of software modularity; see Ref. [11].

The customary approach to bypass these problems is through *segregation*. The fluid and structure equations are then solved alternately subject to complementary partitions of the interface conditions. This iterative process is commonly referred to as subiteration, successive approximation or Picard iteration. The conventional implementation of this method imposes the dynamic interface conditions (tractions) on the structure, and the kinematic interface conditions (displacements) on the fluid; see, for instance, Refs. [1, 5, 16, 18]. The advantage of segregation-based solution methods is the separation of the fluid-structure-interaction problem into two common subproblems, viz., the independent solution of the initial-boundary-value problems associated with the fluid and the structure on prescribed computational domains, and the separate displacement of the sections of the boundaries of the computational domains associated with the interface. The essential disadvantage of these methods pertains to their convergence behaviour. Regularly, convergence is excessively slow, or prohibitively small

time steps are required to maintain stability. Moreover, the operator associated with the subiteration process is generally nonnormal, which yields a severe degradation in the robustness and efficiency of the method; see [7]. Another shortcoming of subiteration is that it precludes reuse of information from previous invocations. In numerical solution procedures for fluid-structure-interaction problems the subiteration method generally operates within a sequential time-integration process. Within each time interval a similar problem is to be solved. Conceptually, a substantial improvement in efficiency can be obtained by reusing information. However, the subiteration method is devoid of any reuse options.

Despite its inadequacy as a solver, the subiteration process provides an apt preconditioner for Krylov-subspace methods such as GMRES [25]. Conversely, the convergence behaviour of the subiteration method can be effectively improved by means of Krylov-subspace acceleration. The characteristics of the subiteration method for fluid-structure-interaction problems endow its conjugation with Krylov-subspace acceleration with many imploring features. Firstly, the subiteration process condenses errors into a low-dimensional space associated with the discrete representation of a function on the interface. Since the Krylov subspace only needs to contain vectors in this space, the acceleration is inexpensive in terms of computational effort and storage. We refer to this process as *Interface-GMRES*. Secondly, the Interface-GMRES-accelerated subiteration method involves several levels of nested iteration and, consequently, numerous reuse options for the Krylov subspace emanate. Thirdly, the subspace acceleration preserves the modularity of the subiteration process. Fourthly, the combined method converges even if the subiteration method itself is unstable. Finally, the subspace acceleration enables underrelaxation without disrupting convergence. Such underrelaxation can be imperative if the subiteration method is unstable, or to mitigate nonnormality-induced divergence.

The acceleration of segregated solution methods for fluid-structure-interaction problems by means of Krylov-subspace methods has received sparse attention in, e.g., Refs. [15, 23]. However, these methods generally treat the segregated solution method as a preconditioner for the aggregated (*monolithic*) equations and, accordingly, the Krylov vectors consist of the aggregated fluid and structure variables, instead of interface variables only. Consequently, these methods are deprived of several of the aforementioned qualities, such as modularity. In Schur-complement-based methods (see, e.g., Ref. [17]) the Schur-complement equation is generally solved by means of a Krylov-subspace method. Because the evaluation of vector products with the Schur complement essentially corresponds to subiteration, these methods are similar to subiteration methods with Krylov-subspace acceleration. However, in conventional implementations the Schur complement acts on the space associated with the discrete representation of the structure, and the dimension of this space is generally much larger than that of the interface space. In [19] the error-amplification behaviour of the subiteration preconditioner is analysed for a linear-algebraic system associated with the discretisation of the aggregated equations. The analysis conveys that the subiteration preconditioner condenses the errors into a subspace of which the dimension N is at most equal to the dimension of the approximation space for the interface displacement. Hence, a Krylov method terminates in at most N steps, independent of the choice of the acceleration space, e.g., aggregated variables, structure variables, or interface variables. However, the computational cost and storage required by the Krylov acceleration itself increase with the dimension of the acceleration space. Therefore, the acceleration on the interface variables proposed in this paper is most efficient. In Ref. [19] it is moreover shown that the Interface-GMRES(R) method can alternatively be construed as a Schur-complement method, as the Krylov acceleration generates an implicit approximation to the Schur complement. In this context, the main difference between the proposed Interface-GMRES(R) method and the Schur-complement method in [17] is the choice of the acceleration space.

The present work investigates Interface-GMRES acceleration of subiteration for fluid-structure-interaction problems. We establish that the subiteration method essentially condenses into a fixed-point iteration for the interface, and we describe the GMRES acceleration of this fixed-point iteration. As the implementation of the GMRES acceleration conforming to [29] typically yields severely ill-conditioned Krylov spaces, we consider intermediate orthonormalisation of the Krylov space, and we prove that the orthonormalisation does not essentially interfere with the convergence of the method.

Furthermore, we examine reuse options for the Krylov spaces, commonly referred to as GMRESR; see [27]. By means of detailed numerical experiments for a prototypical one-dimensional model problem, we illustrate the properties and the potential of GMRES(R) acceleration of the subiteration method.

The contents of this paper are organised as follows: Section 2 presents a generic problem statement. Section 3 describes the subiteration method for fluid-structure-interaction problems. Section 4 is concerned with the Interface-GMRES(R) acceleration of the subiteration method. Numerical experiments and results are presented in Section 5. Finally, Section 6 contains concluding remarks.

2. Problem Statement

To facilitate the ensuing presentation, this section provides a generic variational space/time formulation of fluid-structure-interaction problems.

2.1 Fluid Problem

To formulate the variational problem associated with the fluid, let $x \in \mathbb{R}^d$ and $t \in \mathbb{R}_+$ designate spatial and temporal coordinates, respectively. We consider an open bounded space/time domain $\Omega_\alpha \subset \mathbb{R}^d \times \mathbb{R}_+$. Its boundary consists of the *interface* between the fluid and the structure, Γ_α , and the fixed boundary, $\partial\Omega_\alpha \setminus \Gamma_\alpha$. We associate the interface Γ_α to a specific representation function α in a space of admissible interface representations \mathbb{A} , i.e., to each $\alpha \in \mathbb{A}$ corresponds a $\Gamma(\alpha) := \Gamma_\alpha$ and, accordingly, a $\Omega(\alpha) := \Omega_\alpha$. To enable a treatment of both viscous and inviscid flows, we assume that $\alpha : \Xi \times \mathbb{R}_+ \mapsto \mathbb{R}^d$ ($\Xi \subseteq \mathbb{R}^{d-1}$) and that the mapping $\alpha \mapsto \Gamma_\alpha$ bears the form

$$\Gamma_\alpha = \{(x, t) : x = \alpha(\xi, t), t \in \mathbb{R}_+, \xi \in \Xi \subseteq \mathbb{R}^{d-1}\}. \quad (2.1)$$

Eq. (2.1) specifies the location of any point on the interface explicitly. The corresponding interface velocity, $d\alpha/dt$, reappears as a boundary condition in the initial-boundary-value problem for the fluid. For viscous flows a specification of the boundary velocity forms an appropriate boundary condition. Inviscid flows require only the boundary velocity in the normal direction. Therefore, for inviscid flows a weaker description than (2.1) suffices. For instance, $\alpha : \Xi \times \mathbb{R}_+ \mapsto \mathbb{R}$ can describe the displacement of a reference surface Γ_0 in the direction of its outward unit normal vector according to $\Gamma_\alpha := \{(x, t) + \alpha(x, t)n(x, t) : (x, t) \in \Gamma_0\}$, or it can indicate the interface by a level set through $\Gamma_\alpha := \{(x, t) : \alpha(x, t) = 0\}$.

To each admissible interface Γ_α corresponds an initial-boundary-value problem for the fluid. Let us condense this initial-boundary-value problem into the abstract variational statement: find

$$u \in \mathbb{U}_\alpha : \quad \mathbb{F}_\alpha(v, u) = \mathbb{f}_\alpha(v) \quad \forall v \in \mathbb{V}_\alpha, \quad (2.2)$$

where $\mathbb{F}_\alpha : \mathbb{V}_\alpha \times \mathbb{U}_\alpha \mapsto \mathbb{R}$ and $\mathbb{f}_\alpha : \mathbb{V}_\alpha \mapsto \mathbb{R}$ denote the semi-linear and linear functionals associated with the differential operator and the prescribed data, respectively. The auxiliary conditions are either weakly enforced and incorporated in the functionals, or strongly enforced and incorporated in the spaces \mathbb{U}_α and \mathbb{V}_α . In either case, there is an awkward dependence of the function spaces on the function α , e.g., through the definition of the corresponding inner products $\langle \cdot, \cdot \rangle_{\mathbb{H}(\Omega_\alpha)}$ ($\mathbb{H} = \mathbb{U}, \mathbb{V}$). This dependence prohibits us from casting the fluid-structure-interaction problem into a canonical variational form. However, in general the variational problem (2.2) can be reformulated as

$$u \in \mathbb{U} : \quad \mathbb{F}(v, u, \alpha) = \mathbb{f}(v) \quad \forall v \in \mathbb{V}, \quad (2.3)$$

wherein \mathbb{U} and \mathbb{V} are independent of α . We assume that (2.3) has a unique solution for all $\alpha \in \mathbb{A}$.

If the auxiliary conditions are weakly enforced, then $\mathbb{H}_\alpha := \mathbb{H}(\Omega_\alpha)$ ($\mathbb{H} = \mathbb{U}, \mathbb{V}$) and the function spaces depend on α through the definition of their inner products $\langle \cdot, \cdot \rangle_{\mathbb{H}(\Omega_\alpha)}$. However, following [22] this dependence can be bypassed straightforwardly by embedding the union of all admissible domains in a *security set* $\Sigma \supset \Omega(\mathbb{A})$, and replacing (2.2) by (2.3) with $\mathbb{H} := \mathbb{H}(\Sigma)$. If $\partial\Omega_\alpha$ is Lipschitz for all $\alpha \in \mathbb{A}$, then there generally exists an extension mapping $E : \mathbb{H}(\Omega_\alpha) \mapsto \mathbb{H}(\Sigma)$ such that $Eu|_{\Omega_\alpha} = u$ for

all $u \in \mathbb{H}(\Omega_\alpha)$ and $\|u\|_{\mathbb{H}(\Sigma)} \leq C \|u\|_{\mathbb{H}(\Omega_\alpha)}$ for some constant C independent of u ; see, e.g., [4, Th.1.4.5]. The functionals $f : \mathbb{V} \mapsto \mathbb{R}$ and $F : \mathbb{V} \times \mathbb{U} \times \mathbb{A} \mapsto \mathbb{R}$ in (2.3) can be formulated such that $u = Eu'$ with u' the solution of (2.2).

If the auxiliary conditions are strongly enforced, then $\mathbb{U}_\alpha := \mathbb{U}(\Omega_\alpha, \alpha)$ and $\mathbb{V}_\alpha := \mathbb{V}_0(\Omega_\alpha)$. The explicit dependence of \mathbb{U}_α on α emanates from the dependence of the boundary conditions at Γ_α on α , and the integration of these boundary conditions in the space \mathbb{U}_α . The test space $\mathbb{V}_0(\Omega_\alpha)$ is constrained accordingly. The dependence of $\mathbb{U}_\alpha, \mathbb{V}_\alpha$ on Ω_α can be removed by means of an α -dependent homeomorphic transformation $(\hat{x}, \hat{t}) \in \hat{\Omega} \mapsto (x, t) \in \Omega_\alpha$, where $\hat{\Omega}$ represents a fixed reference domain. Assuming that the transformation is sufficiently regular, any function in $\mathbb{H}(\Omega_\alpha)$ can be represented by a function in $\mathbb{H}(\hat{\Omega})$. Hence, the variational problem (2.2) can be recast into the form:

$$\hat{u} \in \mathbb{U}_\alpha(\hat{\Omega}) : \quad \hat{F}(\hat{v}, \hat{u}, \alpha) = \hat{f}(\hat{v}) \quad \forall \hat{v} \in \mathbb{V}_0(\hat{\Omega}), \quad (2.4)$$

where

$$\mathbb{U}_\alpha(\hat{\Omega}) := \{\hat{u} \in \mathbb{U}(\hat{\Omega}) : \mathbf{A}(\kappa, \hat{u}|_{\hat{\Gamma}}) = \mathbf{a}(\kappa, \alpha) \forall \kappa \in \mathbb{K}\}, \quad (2.5a)$$

$$\mathbb{V}_0(\hat{\Omega}) := \{\hat{v} \in \mathbb{V}(\hat{\Omega}) : \mathbf{B}(\lambda, \hat{v}|_{\hat{\Gamma}}) = \mathbf{b}(\lambda) \forall \lambda \in \mathbb{L}\}. \quad (2.5b)$$

The constraints on the traces in (2.5a) and (2.5b) impose the auxiliary conditions and the corresponding restrictions on the test functions, respectively. The remaining dependence of $\mathbb{U}_\alpha(\hat{\Omega})$ on α can now be disposed of in two manners. Firstly, we can select a $\hat{u}_\alpha \in \mathbb{U}_\alpha(\hat{\Omega})$ and replace $\mathbb{U}_\alpha(\hat{\Omega})$ by $\hat{u}_\alpha + \mathbb{U}_0(\hat{\Omega})$. We then recover (2.3) with $v := \hat{v}$, $u := \hat{u} - \hat{u}_\alpha$, and

$$F(v, u, \alpha) := \hat{F}(v, \hat{u}_\alpha + u, \alpha), \quad f(v) := \hat{f}(v) \quad \mathbb{U} := \mathbb{U}_0(\hat{\Omega}), \quad \mathbb{V} := \mathbb{V}_0(\hat{\Omega}). \quad (2.6)$$

Secondly, we can transfer the constraints in (2.5) to the variational statement. We then recover (2.3) with $u := (\hat{u}, \lambda)$, $v := (\hat{v}, \kappa)$,

$$F(v, u, \alpha) := \hat{F}(\hat{v}, \hat{u}, \alpha) + \mathbf{A}(\kappa, \hat{u}|_{\hat{\Gamma}}) - \mathbf{a}(\kappa, \alpha) + \mathbf{B}(\lambda, \hat{v}|_{\hat{\Gamma}}) - \mathbf{b}(\lambda), \quad f(v) := \hat{f}(\hat{v}), \quad (2.7)$$

and $\mathbb{U} := \mathbb{U}(\hat{\Omega}) \times \mathbb{L}$ and $\mathbb{V} := \mathbb{V}(\hat{\Omega}) \times \mathbb{K}$. The functions κ, λ then act as Lagrange multipliers.

2.2 Structure Problem

The initial-boundary-value problem for the structure subject to prescribed initial conditions and a prescribed stress tensor σ on its boundary can be condensed into the variational statement: find

$$z \in \mathbb{Z} : \quad \mathbf{S}_\sigma(y, z) = \mathbf{s}(y) \quad \forall y \in \mathbb{Y} \quad (2.8)$$

with $\mathbb{Z} := \mathbb{Z}(\Phi)$, $\mathbb{Y} := \mathbb{Y}(\Phi)$, and Φ an open bounded space/time domain, which can be interpreted as a reference configuration. We shall assume that Dirichlet boundary conditions are incorporated in \mathbb{Z} , and that \mathbb{Y} is constrained accordingly. The section of the boundary $\partial\Phi$ that corresponds to the interface is indicated by Θ . For convenience, we assume that the function z represents the space/time position of a point in the reference configuration. In particular, the trace $z|_\Theta$ represents the structure boundary at the interface.

The prescribed stress tensor σ appears in the functional \mathbf{S}_σ instead of the functional \mathbf{s} , which contains the prescribed data, because the tractions on the structure boundary involve inner products of σ with the outward unit normal vector on $z|_{\partial\Phi}$, and this normal vector depends on z .

The stress tensor on the boundary Θ is provided by the fluid, and is unknown a priori; see §2.3. To elucidate this dependence, we introduce the notation $\mathbf{S}(y, z, \pi) := \mathbf{S}_\sigma(y, z)$, where π represents the stress tensor on Θ . The dependence on the stress tensor at $\partial\Phi \setminus \Theta$ is tacitly incorporated in \mathbf{S} . Hence, Eq. (2.8) is replaced by

$$z \in \mathbb{Z} : \quad \mathbf{S}(y, z, \pi) = \mathbf{s}(y) \quad \forall y \in \mathbb{Y}. \quad (2.9)$$

We assume that (2.9) has a unique solution for all π in a space of admissible stress-tensor functions \mathbb{P} .

2.3 Interface Conditions

The fluid problem and the structure problem are interconnected by interface conditions. The interface conditions for the fluid-structure system can be separated into kinematic conditions and dynamic conditions.

The kinematic conditions stipulate that the fluid and structure boundaries coincide at the interface and, moreover, that the fluid velocity at the interface is identical to the velocity of the interface. The latter condition can be straightforwardly imposed as a boundary condition in the initial-boundary-value problem for the fluid (see §2.1) and henceforth we shall assume that it is incorporated in the variational problem (2.3). The former condition interrelates the displacement of the structure at the interface $z|_{\Theta}$ and the representation of the fluid boundary α through the identity $\Gamma_{\alpha} = z|_{\Theta}(\Theta)$. We express this identity through the variational statement

$$\alpha \in \mathbb{A} : \quad \mathbf{K}(s, \alpha, z) = \mathbf{k}(s) \quad \forall s \in \mathbb{S}, \quad (2.10)$$

e.g., if $\alpha = z_0 + z|_{\Theta}$ and $z_0, z|_{\Theta} \in \mathbb{A}$ then $\mathbf{K}(s, \alpha, z) = \langle s, \alpha - z|_{\Theta} \rangle_{\mathbb{A}}$ and $\mathbf{k}(s) = \langle s, z_0 \rangle_{\mathbb{A}}$.

The dynamic condition specifies that the stress tensor π that is imposed on the structure boundary $z|_{\Theta}$ is identical to the stress tensor in the fluid at the boundary Γ_{α} . In general, the fluid stress tensor is an operator on \mathbb{U} conforming to $T : \mathbb{U}(\Omega) \mapsto \mathbb{T}(\Omega) \subset (\Omega \mapsto \mathbb{R}^{d \times d})$, associated with a constitutive relation. An example is the constitutive relation for an inviscid compressible flow $T : u \mapsto p(u)I$, with p a prescribed equation of state and I the identity in $\mathbb{R}^{d \times d}$. Another relevant example is the stress tensor for an incompressible Newtonian fluid $T : (\mathbf{v}, p) \mapsto pI - \text{Re}^{-1}([\nabla \mathbf{v}] + [\nabla \mathbf{v}]^T)$, where $(\mathbf{v}, p) =: u$ connotes a velocity/pressure pair and Re represents the Reynolds number. The dynamic condition stipulates $\pi = T(u)|_{\Gamma_{\alpha}}$. We condense this condition into the variational statement

$$\pi \in \mathbb{P} : \quad \mathbf{D}(w, u, \alpha, \pi) = 0 \quad \forall w \in \mathbb{W}. \quad (2.11)$$

For instance, if $T(u)|_{\Gamma_{\alpha}} \in \mathbb{P}$ then $\mathbf{D}(w, u, \alpha, \pi) = \langle w, \pi - T(u)|_{\Gamma_{\alpha}} \rangle_{\mathbb{P}}$.

2.4 Aggregated Variational Problem

With the above definitions, the fluid-structure-interaction problem in space/time can be condensed into the canonical form: find

$$\varphi \in \mathbb{F} : \quad \mathbf{P}(\gamma, \varphi) = \mathbf{p}(\gamma) \quad \forall \gamma \in \mathbb{G}. \quad (2.12a)$$

Herein, φ is the quadruple $\varphi := (u, \alpha, z, \pi)$ in the product space $\mathbb{F} := \mathbb{U} \times \mathbb{A} \times \mathbb{Z} \times \mathbb{P}$, the test space consists of the quadruples $\gamma := (v, s, y, w)$ in the product space $\mathbb{G} := \mathbb{V} \times \mathbb{S} \times \mathbb{Y} \times \mathbb{W}$, and the aggregated functionals $\mathbf{P} : \mathbb{F} \times \mathbb{G} \mapsto \mathbb{R}$ and $\mathbf{p} : \mathbb{G} \mapsto \mathbb{R}$ are defined as

$$\mathbf{P}((v, s, y, w), (u, \alpha, z, \pi)) := \mathbf{F}(v, u, \alpha) + \mathbf{S}(y, z, \pi) + \mathbf{K}(s, \alpha, z) + \mathbf{D}(w, u, \alpha, \pi), \quad (2.12b)$$

$$\mathbf{p}((v, s, y, w)) := \mathbf{f}(v) + \mathbf{s}(y) + \mathbf{k}(s). \quad (2.12c)$$

For an instance of a variational formulation of a fluid-structure-interaction problem conforming to (2.12) see Ref. [8]. Sufficient conditions for the existence of a unique solution to variational problems of the generic form (2.12) follow from the generalised nonlinear Lax-Milgram theorem; cf., e.g., Ref. [7].

2.5 Finite-Element Discretisation

The finite-element discretisation of the fluid-structure-interaction problem (2.12) can be formulated straightforwardly by replacing \mathbb{F} and \mathbb{G} by the finite-dimensional subspaces $\tilde{\mathbb{F}}$ and $\tilde{\mathbb{G}}$ associated with the finite-element approximation. Upon introducing bases $\{\hat{\varphi}_i\}_{i=1}^N$ and $\{\hat{\gamma}_i\}_{i=1}^N$ for $\tilde{\mathbb{F}}$ and $\tilde{\mathbb{G}}$ ($N = \dim(\tilde{\mathbb{F}}) = \dim(\tilde{\mathbb{G}})$), Eq. (2.12a) yields a system of nonlinear algebraic equations for the coefficients $\{\check{\varphi}_i\}$ of the solution with respect to $\{\hat{\varphi}_i\}$ according to $\mathbf{P}(\hat{\gamma}_i, \sum \check{\varphi}_j \hat{\varphi}_j) =: P_i(\check{\varphi}_1, \dots, \check{\varphi}_N) = p_i := \mathbf{p}(\hat{\gamma}_i)$.

It is important to note that in general the dimensions of the approximation spaces $\tilde{\mathbb{A}}$ and $\tilde{\mathbb{P}}$ are negligible compared to the dimensions of $\tilde{\mathbb{U}}$ and $\tilde{\mathbb{Z}}$, because α and π refer to boundary functions. More precisely, if $\mathcal{D}(\mathbb{H})$ represents the domain of functions in \mathbb{H} , then $\text{codim}\mathcal{D}(\tilde{\mathbb{A}}) = \text{codim}\mathcal{D}(\tilde{\mathbb{P}}) = 1$.

3. Subiteration for Fluid-Structure-Interaction Problems

The simultaneous (*monolithic*) solution of the aggregated fluid-structure-interaction problem (2.12) is complicated by the inherent interdependence of the fluid and structure state variables and their domains of definition. The conventional approach to bypass these complications is through a segregation-based iterative approach referred to as subiteration. In this section, we first examine the problems pertaining to the application of Newton's method to fluid-structure-interaction problems. We then consider the subiteration method.

3.1 Newton's Method

To describe Newton's method for a nonlinear variational problem of the generic form (2.12a), let us specify the Fréchet derivative of the functional $P : \mathbb{G} \times \mathbb{F} \mapsto \mathbb{R}$ with respect to its nonlinear argument. For any fixed $\gamma_0 \in \mathbb{G}$, $P(\gamma_0, \cdot)$ is a nonlinear functional on \mathbb{F} . The functional $P(\gamma_0, \cdot)$ is Fréchet differentiable at $\varphi_0 \in \mathbb{F}$ if there exists a bounded linear functional $P'(\gamma_0, \varphi_0, \cdot) : \mathbb{F} \mapsto \mathbb{R}$ such that

$$\lim_{\varphi' \rightarrow 0} \frac{|P(\gamma_0, \varphi_0 + \varphi') - P(\gamma_0, \varphi_0) - P'(\gamma_0, \varphi_0, \varphi')|}{\|\varphi'\|_{\mathbb{F}}} = 0. \quad (3.1)$$

The functional $P'(\gamma_0, \varphi_0, \cdot)$ is then called the Fréchet derivative of P to φ at (γ_0, φ_0) . Assuming that the functional $P'(\gamma, \varphi, \cdot)$ exists for all $\gamma \in \mathbb{G}$, $\varphi \in \mathbb{F}$, we identify P' with a functional on $\mathbb{G} \times \mathbb{F} \times \mathbb{F}$. With this definition of the derivative P' , and provided with an initial approximation $\varphi_0 \in \mathbb{F}$, Newton's method for the variational problem (2.12a) is defined as the following iterative process: for $j = 1, 2, \dots$, find

$$\varphi_j \in \mathbb{F} : \quad P'(\gamma, \varphi_{j-1}, \varphi_j - \varphi_{j-1}) = p(\gamma) - P(\gamma, \varphi_{j-1}) \quad \forall \gamma \in \mathbb{G}. \quad (3.2)$$

If the initial estimate φ_0 is sufficiently close to the actual solution, then φ_j converges to the solution of the variational problem as $j \rightarrow \infty$.

To elucidate the complications of Newton's method for fluid-structure-interaction problems, let us expand the derivative P' :

$$\begin{aligned} P'(\gamma, \varphi, \varphi') := & F'_u(v, u, \alpha, u') + F'_\alpha(v, u, \alpha, \alpha') + S'_z(y, z, \pi, z') + S'_\pi(y, z, \pi, \pi') + K'_\alpha(s, \alpha, z, \alpha') \\ & + K'_z(s, \alpha, z, z') + D'_u(w, u, \alpha, \pi, u') + D'_\alpha(w, u, \alpha, \pi, \alpha') + D'_\pi(w, u, \alpha, \pi, \pi'). \end{aligned} \quad (3.3)$$

In Eq. (3.3) we use the notation G'_g to indicate the Fréchet derivative of a functional G with respect to its argument g . The first problem concerns the *shape derivative* F'_α , induced by the interdependence of the fluid-state variables and their domain of definition. Discrete approximation methods, e.g., finite elements, customarily employ boundary fitted meshes. As a perturbation of the interface generally yields a deformation of the mesh throughout the entire computational domain, F'_α behaves as a nonlocal operator. This renders the computational expenses incurred in the evaluation of the shape derivative F'_α prohibitive in actual applications. It is to be remarked, however, that in specific cases the problems pertaining to the shape derivatives can be mitigated by workarounds such as the method of spines; see, e.g., Refs. [15, 26]. A second problem is the inherent interconnection between the fluid and the structure, induced by the derivatives of the interface conditions. The functionals D and K depend on the arguments u, α , associated with the fluid, as well as on z, π , corresponding to the structure. This is illustrated in Table 1. Hence, the matrix \mathbf{P} associated with a discrete approximation of the operator P' in (3.2) is inseparable and the fluid and structure equations must be resolved simultaneously. This has severe practical disadvantages, such as the loss of modularity; see [11]. The third problem concerns the fact that the matrix \mathbf{P} is generally severely ill-conditioned due to the disparate properties of the initial-boundary-value problems of the fluid and the structure. Moreover, the entries in \mathbf{P} that emanate from the interface conditions often compound the ill-conditioning. This ill-conditioning forms a severe asperity for iterative solution methods. On the other hand, for practical fluid-structure-interaction problems the computational cost of direct methods is prohibitive.

	α	u	π	z
K	\times	0	0	\times
F	\times	\times	0	0
D	\times	\times	\times	0
S	0	0	\times	\times

Table 1: Illustration of the connectivity in fluid-structure-interaction problems.

3.2 Subiteration

Many of the complications of Newton's method can be avoided by means of a segregation-based iterative approach, commonly referred to as *subiteration* or, alternatively, Picard iteration or successive approximation. Provided with an initial approximation $z_0 \in \mathbb{Z}$ of the structure solution or, in particular, of the structure displacement at the interface $(z|_{\Theta})_0$, the following iterative process defines the subiteration algorithm: for $j = 1, 2, \dots$, repeat

- (S1) Solve the kinematic condition: find $\alpha_j \in \mathbb{A}$ such that $\mathbf{K}(s, \alpha_j, z_{j-1}) = \mathbf{k}(s)$ for all $s \in \mathbb{S}$.
- (S2) Solve the fluid: find $u_j \in \mathbb{U}$ such that $\mathbf{F}(v, u_j, \alpha_j) = \mathbf{f}(v)$ for all $v \in \mathbb{V}$.
- (S3) Solve the dynamic condition: find $\pi_j \in \mathbb{P}$ such that $\mathbf{D}(w, u_j, \alpha_j, \pi_j) = 0$ for all $w \in \mathbb{W}$.
- (S4) Solve the structure: find $z_j \in \mathbb{Z}$ such that $\mathbf{S}(y, z_j, \pi_j) = \mathbf{s}(y)$ for all $y \in \mathbb{Y}$.

It is to be noted that this procedure obviates the computation of the shape derivative, and the simultaneous treatment of the fluid and the structure. Operations (S2) and (S4) involve the solution of standard problems, viz., the solution of a fluid problem on a prescribed domain subject to prescribed auxiliary conditions, and the solution of a structure problem subject to prescribed auxiliary conditions. Operations (S1) and (S3) involve the solution of projection problems. The computational cost of these operations is negligible on account of the negligibility of $\dim(\mathbb{A}) + \dim(\tilde{\mathbb{P}})$, corresponding to the discrete representation of the displacement and traction on the interface, compared to $\dim(\tilde{\mathbb{U}}) + \dim(\tilde{\mathbb{Z}})$, corresponding to the discrete representation of the fluid and structure state variables.

The subiteration method conforms to the *defect correction* paradigm [3]. The defect correction method for the generic variational problem (2.12a) is defined by the following iterative process: given an initial approximation $\varphi_0 \in \mathbb{F}$, for $j = 1, 2, \dots$ find

$$\varphi_j \in \mathbb{F} : \quad \tilde{\mathbf{P}}(\gamma, \varphi_j) = \mathbf{p}(\gamma) - (\mathbf{P}(\gamma, \varphi_{j-1}) - \tilde{\mathbf{P}}(\gamma, \varphi_{j-1})) \quad \forall \gamma \in \mathbb{G}, \quad (3.4)$$

where $\tilde{\mathbf{P}} : \mathbb{G} \times \mathbb{F} \mapsto \mathbb{R}$ represents an appropriate approximation to \mathbf{P} . The term in parenthesis in the right member is referred to as the *defect*. A suitable initial approximation is $\varphi_0 \in \mathbb{F}$ such that $\tilde{\mathbf{P}}(\gamma, \varphi_0) = \mathbf{p}(\gamma)$ for all $\gamma \in \mathbb{G}$. If $\tilde{\mathbf{P}}$ is sufficiently close to \mathbf{P} , then φ_j approaches the solution of (2.12a) as $j \rightarrow \infty$. To determine the approximate functional associated to the subiteration method, we note that the approximations generated by (S1)–(S4) satisfy

$$\mathbf{F}(v, u_j, \alpha_j) + \mathbf{S}(y, z_j, \pi_j) + \mathbf{K}(s, \alpha_j, z_{j-1}) + \mathbf{D}(w, u_j, \alpha_j, \pi_j) = \mathbf{f}(v) + \mathbf{s}(y) + \mathbf{k}(s) \quad (3.5)$$

for all admissible (v, s, y, w) . In general, the functional \mathbf{K} is linear on $\mathbb{S} \times \mathbb{A} \times \mathbb{Z}$ and separable in \mathbb{A} and \mathbb{Z} , i.e., $\mathbf{K}(s, \alpha, z) = \mathbf{K}_0(s, \alpha) + \mathbf{K}_1(s, z)$. We then immediately recover (3.4) with the approximate functional

$$\tilde{\mathbf{P}}((v, s, y, w), (u, \alpha, z, \pi)) := \mathbf{F}(v, u, \alpha) + \mathbf{S}(y, z, \pi) + \mathbf{K}(s, \alpha, \bar{z}) + \mathbf{D}(w, u, \alpha, \pi) \quad (3.6)$$

with \bar{z} any fixed element of \mathbb{Z} . It is to be noted that the approximation only involves the functional \mathbf{K} corresponding to the kinematic interface condition. The connectivity table associated with

the approximate operator is identical to Table 1, but with the right-upper (\mathbf{K}, z) -entry eliminated. Hence, the connectivity table is lower triangular, and the subproblems involving the inversion of the approximate operator $\tilde{\mathbf{P}}$ can be solved conveniently by forward substitution. From this perspective the subiteration method can be conceived as a block Gauss-Seidel method.

The segregation that underlies the subiteration method can alternatively be invoked in the linearised problem (3.2); see, e.g., Ref. [15]. The linear variational problem (3.2) in Newton's method is then replaced by

$$\varphi_j \in \mathbb{F}: \quad \tilde{\mathbf{P}}'(\gamma, \varphi_{j-1}, \varphi_j - \varphi_{j-1}) = \mathbf{p}(\gamma) - \mathbf{P}(\gamma, \varphi_{j-1}) \quad \forall \gamma \in \mathbb{G}. \quad (3.7)$$

The Jacobian matrix associated with $\tilde{\mathbf{P}}'$ is lower triangular and (3.7) can be solved by forward substitution. However, such a linear subiteration approach is inept, because it reintroduces the shape derivatives in the linear variational subproblem: find $u_j \in \mathbb{U}$ such that

$$\mathbf{F}'_\alpha(v, u_{j-1}, \alpha_{j-1}, \alpha_j - \alpha_{j-1}) + \mathbf{F}'_u(v, u_{j-1}, \alpha_{j-1}, u_j - u_{j-1}) = \mathbf{f}(v) - \mathbf{F}(v, u_{j-1}, \alpha_{j-1}) \quad \forall v \in \mathbb{V}. \quad (3.8)$$

The shape derivatives can however be avoided by a minor modification of (3.8). Noting that in the forward substitution process α_j is determined before u_j , the first term in (3.8) can be transferred to the right-hand side. On account of (3.1), it holds that

$$\mathbf{F}(v, u_{j-1}, \alpha_{j-1}) + \mathbf{F}'_\alpha(v, u_{j-1}, \alpha_{j-1}, \alpha_j - \alpha_{j-1}) = \mathbf{F}(v, u_{j-1}, \alpha_j) + o(\|\alpha_j - \alpha_{j-1}\|) \quad (3.9)$$

as $\|\alpha_j - \alpha_{j-1}\| \rightarrow 0$. As terms of $o(\|\varphi_j - \varphi_{j-1}\|)$ are ignored in the Newton process, Eq. (3.8) can be replaced by

$$\mathbf{F}'_u(v, u_{j-1}, \alpha_{j-1}, u_j - u_{j-1}) = \mathbf{f}(v) - \mathbf{F}(v, u_{j-1}, \alpha_j) \quad (3.10)$$

without any additional suppositions. In fact, α_{j-1} in the left member of (3.10) can be replaced by α_j as well. Eq. (3.10) can then be identified as a Newton iteration for the fluid problem corresponding to the modified interface representation α_j .

Finally, it is to be noted that (S1)–(S4) describes the subiteration method in terms of the *continuum* problem, i.e., we conceive of the function spaces in (S1)–(S4) as the (generally infinite-dimensional) Hilbert spaces that furnish the setting of (2.12). Of course, in practice, these function spaces are replaced by finite-dimensional subspaces corresponding to, for instance, a finite-element approximation, and each of the substeps (S1)–(S4) is solved numerically. However, the fact that the method admits a continuum description implies that its convergence behaviour is asymptotically independent of the mesh width and order of the approximation spaces, i.e., the convergence behaviour of the subiteration method is identical for all sufficiently fine discretisations.

4. Interface-GMRES(R) Acceleration

This section is concerned with the acceleration of subiteration by means of GMRES. §4.1 presents the Interface-GMRES acceleration of the subiteration process. The Interface-GMRES method with intermediate orthonormalisation is described in §4.2. Finally, §4.3 explores the reuse options that issue from the several levels of nested iteration in the subiteration method with Interface-GMRES-accelerated subiteration method.

4.1 GMRES Acceleration of Interface Fixed-Point Iterations

The subiteration method induces a mapping $z_{j-1} \mapsto z_j$ or, more precisely, $(z|_\Theta)_{j-1} \mapsto (z|_\Theta)_j$. Alternatively, we can consider cyclic permutations of the operations (S1)–(S4) and conceive the subiteration method as a map $\alpha_{j-1} \mapsto \alpha_j$, $u_{j-1} \mapsto u_j$ or $\pi_{j-1} \mapsto \pi_j$. Accordingly, the subiteration method can be condensed into a fixed-point iteration $\beta_j = \Lambda \beta_{j-1}$ with $\beta \in \{z, z|_\Theta, \alpha, u, \pi\}$ and Λ a nonlinear automorphic operator on \mathbb{B} . There is an immediate correspondence between the convergence of these fixed-point iterations and the convergence of the subiteration method, i.e., if φ^* represents the solution of (2.12), then $\|\varphi_{j+1} - \varphi^*\|_{\mathbb{F}} \leq \text{const} \|\beta_j - \beta^*\|_{\mathbb{B}}$ with $\|\cdot\|_{\mathbb{B}}$ the appropriate norm for β . Conversely,

the convergence of the subiteration method can be improved by accelerating the convergence of any of the fixed-point iterations.

Let us now consider the GMRES acceleration of the generic fixed-point iteration $\beta_j = \Lambda\beta_{j-1}$. The general methodology is standard; see, e.g., Refs. [6, 29]. We define the residual operator $R: \beta \in \mathbb{B} \mapsto \Lambda\beta - \beta \in \mathbb{B}$. Clearly, $R\beta^* = 0$ is equivalent to β^* being a fixed point. We consider a sequence of iterates $\{\beta_i\}_{i=0}^{i=n}$ and corresponding residuals $\{r_i\}_{i=0}^{i=n}$, i.e., $r_i := R\beta_i = \beta_{i+1} - \beta_i$. Based on these sequences we construct a sequence of search directions with elements $\beta'_i := \beta_i - \beta_0$ and a corresponding sequence of residual sensitivities with elements $r'_i := r_i - r_0$. For any particular $\beta \in \beta_0 + \text{span}\{\beta'_i\}_{i=1}^{i=n}$ there exist coefficients $\{\theta_i\}_{i=1}^{i=n} =: \boldsymbol{\theta} \in \mathbb{R}^n$ such that $\beta = \beta_0 + \sum \theta_i \beta'_i$. For the corresponding residual it holds that

$$\begin{aligned} R(\beta_0 + \sum \theta_i \beta'_i) &= R\beta_0 + \sum \theta_i R'(\beta_0)\beta'_i + o(\sum \|\theta_i \beta'_i\|_{\mathbb{B}}) \\ &= R\beta_0 + \sum \theta_i (R\beta_i - R\beta_0) + o(\sum \|\theta_i \beta'_i\|_{\mathbb{B}}) = r_0 + \sum \theta_i r'_i + o(\sum \|\theta_i \beta'_i\|_{\mathbb{B}}), \end{aligned} \quad (4.1)$$

as $\sum \|\theta_i \beta'_i\|_{\mathbb{B}} \rightarrow 0$, where $R'(\beta_0)$ denotes the Fréchet derivative of R at β_0 . Therefore, on linear approximation, i.e., ignoring the o -terms in (4.1), if we determine the coefficients from

$$\bar{\boldsymbol{\theta}} = \arg \min_{\boldsymbol{\theta} \in \mathbb{R}^n} \|r_0 + \sum \theta_i r'_i\|_{\mathbb{B}}, \quad (4.2)$$

then $\beta_0 + \sum \bar{\theta}_i \beta'_i$ is the minimiser of $\|R(\cdot)\|_{\mathbb{B}}$ in $\beta_0 + \text{span}\{\beta'_i\}_{i=1}^{i=n}$.

In a numerical computation, the space \mathbb{B} is replaced by a suitable finite-dimensional approximation $\tilde{\mathbb{B}}$. The minimisation problem (4.2) then gives rise to a least-squares problem, the computational cost of which is typically proportional to $n^2 \dim(\tilde{\mathbb{B}})$; see, e.g., Ref. [12, p.238 ff.]. Moreover, the storage for $\{\beta'_i\} \subset \tilde{\mathbb{B}}$ and $\{r'_i\} \subset \tilde{\mathbb{B}}$ is also proportional to $\dim(\tilde{\mathbb{B}})$. Computational cost and storage can thus be minimised by selecting for $\tilde{\mathbb{B}}$ the approximation space with the lowest dimension. This is in general one of the interface approximation spaces $\tilde{\mathbb{A}}, \tilde{\mathbb{P}}$ or $\{z|_{\Theta} : z \in \tilde{\mathbb{Z}}\}$. It is to be noted that such an Interface-GMRES-acceleration procedure retains the modularity of the underlying subiteration method.

The Interface-GMRES procedure is summarised in Algorithm 1. The operator Λ represents the mapping induced by the subiteration process, the parameters ϵ_0, ϵ_1 ($0 < \epsilon_1 \leq \epsilon_0$) are suitable tolerances, and ζ acts as a residual estimator. Note that the solution quadruple (u, α, z, π) can be extracted immediately from the operation $\beta_1 = \Lambda\beta_0$ on line 1 or line 13 of the algorithm.

```

1:  $j = 0; \beta_1 = \Lambda\beta_0; r_j = \beta_1 - \beta_0;$ 
2: while  $\|r_j\|_{\mathbb{B}} > \epsilon_0$  do
3:    $\zeta = \|r_j\|_{\mathbb{B}}; i = 0;$ 
4:   while  $\zeta > \epsilon_1$  do
5:      $i = i + 1;$ 
6:      $\beta'_i = \beta_i - \beta_0;$ 
7:      $\beta_{i+1} = \Lambda\beta_i;$ 
8:      $r'_i = (\beta_{i+1} - \beta_i) - r_j;$ 
9:      $\bar{\boldsymbol{\theta}} = \arg \min \|r_j + \sum_{k=1}^{k=i} \theta_k r'_k\|_{\mathbb{B}};$ 
10:     $\zeta = \|r_j + \sum_{k=1}^{k=i} \bar{\theta}_k r'_k\|_{\mathbb{B}};$ 
11:   end while
12:    $\beta_0 = \beta_0 + \sum_{k=1}^{k=i} \bar{\theta}_k \beta'_k;$ 
13:    $j = j + 1; \beta_1 = \Lambda\beta_0; r_j = \beta_1 - \beta_0;$ 
14: end while
```

Algorithm 1: The Interface-GMRES-accelerated subiteration method.

The above exposition presents the Interface-GMRES method as an acceleration method for the interface fixed-point iteration induced by subiteration. We remark that the method admits an al-

ternative interpretation: The subiteration method constitutes a preconditioner for the *aggregated* system, and the Interface-GMRES-acceleration method solves this preconditioned aggregated system by means of a Krylov method; see [19]. The error-amplification analysis in [19] conveys that indeed the subiteration preconditioner condenses errors into a subspace which can be associated with the interface variables. Accordingly, the Krylov vectors for the aggregated system can be represented in the interface approximation space.

On linear approximation, the Interface-GMRES-acceleration method corresponds to an application of GMRES to a linear system with operator $R' = \Lambda' - I$. Hence, to assess convergence of the method, one can apply the usual GMRES convergence bounds; cf., for instance, Ref. [13]. In this context, it is important to mention that the operator $\Lambda' - I$ can be nonnormal (see, for example, Ref. [7] and Sec. 5), as nonnormality of the operator can degrade the sharpness of certain GMRES convergence bounds. Convergence bounds for a prototypical fluid-structure-interaction problem are provided in Ref. [19].

Finally, it is to be noted that the description of the Interface-GMRES-accelerated subiteration method in Algorithm 1 conceives of the operator Λ as a *continuum* operator, i.e., the operator pertaining to the continuum description of the subiteration process; see §3.2. By the same arguments as in §3.2, it follows that if the method is applied to a discrete approximation of a fluid-structure-interaction problem, then its convergence behaviour is identical for all sufficiently fine discretisations.

4.2 Orthonormalisation of the Krylov Space

The robustness of the Interface-GMRES-accelerated subiteration process in Algorithm 1 can be substantially improved by intermediate orthonormalisation of the vectors in $\{\beta'_i\}$. In finite precision arithmetic, the accuracy of the solution of (4.2) deteriorates quadratically with the condition number of the basis $\{r'_i\}$; see [12, §5.3.7-8]. In general, orthonormalisation of $\{\beta'_i\}$ yields an according improvement in the condition of $\{r'_i\}$. Moreover, the orthonormalisation imposes $\|\beta_i\|_{\mathbb{B}} \leq \|\beta_0\|_{\mathbb{B}} + \nu$ with ν some suitable constant. Contrastingly, in the basic subiteration method and, accordingly, in Algorithm 1 the norm $\|\beta_i\|_{\mathbb{B}}$ can increase indefinitely if the iteration $\beta_i = \Lambda\beta_{i-1}$ diverges, e.g., due to nonnormality (see Ref. [7]) or instability.

The orthonormalisation can be accomplished by standard techniques such as the Gram-Schmidt procedure. The conjunction with the subiteration process involves a redefinition of the iterate β_i according to $\beta_i = \beta_0 + \beta'_i$ after the orthonormalisation of β'_i . The Interface-GMRES-accelerated subiteration method with Gram-Schmidt orthonormalisation is obtained by replacing line 6 in Algorithm 1 by the instructions in Algorithm 2. One can infer that the corresponding basis $\{\beta'_i\}$ is orthogonal. Moreover, it holds that $\|\beta'_i\|_{\mathbb{B}} = \nu$ and, hence, $\|\beta_i\|_{\mathbb{B}} = \|\beta_0 + \beta'_i\|_{\mathbb{B}} \leq \|\beta_0\|_{\mathbb{B}} + \nu$ by Schwarz' inequality. As the parameter ν determines the norm of the update, it can be conceived as an underrelaxation parameter.

```

6a:  $\beta'_i = \beta_i - \beta_0$ ;
6b: for  $k = 1 : i - 1$  do
6c:    $\beta'_i = \beta'_i - \beta'_k \langle \beta'_i, \beta'_k \rangle_{\mathbb{B}} / \|\beta'_k\|_{\mathbb{B}}^2$ ;
6d: end for
6e:  $\beta'_i = \nu \beta'_i / \|\beta'_i\|_{\mathbb{B}}$ ;
6f:  $\beta_i = \beta_0 + \beta'_i$ ;

```

Algorithm 2: Modification of the Interface-GMRES method: Gram-Schmidt orthonormalisation and subsequent redefinition of β_i .

To demonstrate that the orthonormalisation does not essentially interfere with the convergence of the accelerated subiteration method, we establish that the search spaces with and without orthonormalisation are asymptotically similar. For this purpose, let $\{\beta'_i\}_{i=1}^{i=n}$ and $\{b'_i\}_{i=1}^{i=n}$ represent the sequences of search directions obtained with and without orthonormalisation, respectively. On ac-

count of $\beta'_1 = \nu b'_1 / \|b'_1\|_{\mathbb{B}}$ it holds that $\text{span}\{\beta'_1\} = \text{span}\{b'_1\}$. Hence, the spaces are identical for $n = 1$. The proof for general n follows straightforwardly by induction: $\text{span}\{\beta'_i\}_{i=1}^{i=n} \sim \text{span}\{b'_i\}_{i=1}^{i=n}$ for some n implies that there are coefficients $\{c_i^n\}_{i=1}^{i=n}$ such that $b'_n = \sum c_i^n \beta'_i + o$, where o connotes terms of $o(\sum \|\beta'_i\|_{\mathbb{B}} + \sum \|b'_i\|_{\mathbb{B}})$ as $\sum \|\beta'_i\|_{\mathbb{B}} + \sum \|b'_i\|_{\mathbb{B}} \rightarrow 0$. Hence,

$$\begin{aligned} b'_{n+1} &= \Lambda(\beta_0 + b'_n) - \beta_0 = \Lambda\left(\beta_0 + \sum_{i=1}^{i=n} c_i^n \beta'_i + o\right) - \beta_0 \sim \beta'_1 + \sum_{i=1}^{i=n} c_i^n (\Lambda(\beta_0 + \beta'_i) - \Lambda(\beta_0)) \\ &= \beta'_1 + \sum_{i=1}^{i=n} c_i^n \sum_{j=1}^{j=n+1} a_j \beta'_j \in \text{span}\{\beta'_i\}_{i=1}^{i=n+1}, \end{aligned} \quad (4.3)$$

for certain coefficients $\{a_i\}_{i=1}^{i=n+1}$. The converse, $\beta'_{n+1} \in \text{span}\{b'_i\}_{i=1}^{i=n+1}$, can be demonstrated in a similar manner. Thus $\text{span}\{b'_i\}_{i=1}^{i=n} \sim \text{span}\{\beta'_i\}_{i=1}^{i=n}$ implies $\text{span}\{b'_i\}_{i=1}^{i=n+1} \sim \text{span}\{\beta'_i\}_{i=1}^{i=n+1}$. This proves that the search spaces with and without orthonormalisation are asymptotically similar.

4.3 Reuse Options: Interface-GMRESR

To facilitate the ensuing presentation, we construe Algorithms 1-2 as hybrid Newton/Krylov methods for the residual equations $R\beta = \Lambda\beta - \beta = 0$; cf. Ref. [6]. Newton's method for $R\beta = 0$ updates an initial approximation β_0 according to $\beta_0 := \beta_0 + \delta$, with δ the solution of the linear system $R'(\beta_0)\delta = -R\beta_0$. The Krylov subspace associated with this linear system is

$$\mathcal{K}_n = \text{span}\{R\beta_0, R'(\beta_0)R\beta_0, \dots, (R'(\beta_0))^{n-1}R\beta_0\}. \quad (4.4)$$

Our objective is to show that $\mathcal{K}_n \sim \text{span}\{\beta'_i\}_{i=1}^{i=n}$ or, equivalently, $\mathcal{K}_n \sim \text{span}\{b'_i\}_{i=1}^{i=n}$. The inner loop and outer loop of Algorithms 1-2 can then be identified as a Krylov method for the linear system and an update of the residual, respectively. On account of $R\beta_0 = \Lambda\beta_0 - \beta_0 = \beta_1 - \beta_0 = b'_1$ it holds indeed that $\mathcal{K}_n = \text{span}\{b'_i\}_{i=1}^{i=n}$ for $n = 1$. The proof for general n follows straightforwardly by induction: $\mathcal{K}_n \sim \text{span}\{b'_i\}_{i=1}^{i=n}$ for some n implies that there are coefficients $\{c_i^n\}_{i=1}^{i=n}$ such that $(R'(\beta_0))^{n-1}R\beta_0 = \sum c_i^n b'_i + o$ with $o := o(\sum \|b'_i\|_{\mathbb{B}})$. Hence,

$$\begin{aligned} (R'(\beta_0))^n R\beta_0 &= R'(\beta_0)(R'(\beta_0))^{n-1}R\beta_0 = R'(\beta_0) \sum_{i=1}^n c_i^n b'_i + o \sim \sum_{i=1}^n c_i^n (R(\beta_0 + b'_i) - R\beta_0) \\ &= \sum_{i=1}^n c_i^n ((\beta_{i+1} - \beta_i) - (\beta_1 - \beta_0)) = \sum_{i=1}^n c_i^n (b'_{i+1} - b'_i - b'_1) \in \text{span}\{b'_i\}_{i=1}^{i=n+1}. \end{aligned} \quad (4.5)$$

Thus, $\mathcal{K}_n \sim \text{span}\{b'_i\}_{i=1}^{i=n}$ implies $\mathcal{K}_{n+1} \sim \text{span}\{b'_i\}_{i=1}^{i=n+1}$. This proves that $\text{span}\{b'_i\}_{i=1}^{i=n}$ and the Krylov space \mathcal{K}_n are asymptotically similar.

In numerical solution procedures for fluid-structure-interaction problems the hybrid Newton/Krylov method generally operates within a sequential time-integration process. Within each time interval of the time-integration process a nonlinear problem of the form $R\beta = 0$ is to be solved. The solution of each of these nonlinear problems by Newton's method requires the solution of several linear problems of the form $R'\delta = -R$. Consequently, the solution of such a linear system is a frequent task in the time-integration process. The Jacobian matrix R' in each of the aforementioned linear problems is distinct: the matrix $R' := R'(\beta_0)$ depends on the active approximation β_0 in the Newton iteration. Furthermore, the residual operator R and, accordingly, its derivative R' are distinct for each time interval, for instance, as a result of differences in initial conditions. Nevertheless, the matrices expectedly exhibit a certain similarity. If the matrices are sufficiently similar, then the subspaces $\text{span}\{\beta'_i\}$ and $\text{span}\{r'_i\}$ can be reused. Such reuse of a Krylov subspace in the successive solution of a sequence of similar linear problems by means of GMRES is referred to as GMRESR; see[27, 28]. The Interface-GMRESR method is derived from Algorithms 1-2 by exchanging the statements on lines 2 and 3, and providing the algorithm with an additional residual estimation between lines 13 and 14.

The modifications are summarised in Alg. 3. The inner loop then augments instead of overwrites the available sequences $\{\beta'_i\}$ and $\{r'_i\}$. The auxiliary residual estimation approximates the reduction of the new nonlinear residual in the already available space of residual sensitivities. The reuse option can be exerted locally within the Newton iteration or globally within the time-integration process. In the latter case, the sequences of search directions and residual sensitivities are transferred from one time interval to the next.

```

2:  $\zeta = \|r_0\|_{\mathbb{B}}; i = 0;$ 
3: while  $\|r_j\|_{\mathbb{B}} > \epsilon_0$  do
     $\vdots$ 
13a:  $j = j + 1; \beta_{i+1} = \Lambda\beta_0; r_j = \beta_{i+1} - \beta_0;$ 
13b:  $\bar{\theta} = \arg \min \|r_j + \sum_{k=1}^{k=i} \theta_k r'_k\|_{\mathbb{B}};$ 
13c:  $\zeta = \|r_j + \sum_{k=1}^{k=i} \bar{\theta}_k r'_k\|_{\mathbb{B}};$ 
14: end while

```

Algorithm 3: The Interface-GMRESR method: modifications of Algorithms 1–2 to exercise the reuse option within the Newton process.

It is to be remarked that the reuse option offers the potential for a significant improvement in the efficiency of the Interface-GMRES method at the expense of robustness: if the derivative $R'(\beta_0)$ corresponding to the active residual operator R and approximation β_0 is too disparate from the derivative(s) underlying the sequence $\{r'_i\}$, then the nonlinear updates can be ineffective, or the residual estimate ζ can stall, despite proper convergence of a method without reuse. The latter defect can be attributed to a rotation of the image of $\{\beta'_i\}$ under the active derivative compared to $\{r'_i\}$. To elucidate this, let us suppose that the residual $R(\beta_0)$ can be effectively reduced in the space $R'(\beta_0) \text{span}\{\beta'_i\}$ ($i = 1, \dots, n$), i.e.,

$$\zeta' := \min_{\theta \in \mathbb{R}^n} \|R(\beta_0) + \sum_{i=1}^{i=n} \theta_i R'(\beta_0) \beta'_i\|_{\mathbb{B}} \quad (4.6)$$

is appropriately small. However, if $R'(\beta_0) \text{span}\{\beta'_i\}$ is rotated compared to $\{r'_i\}$, then the residual estimate ζ in Alg. 3 need not be small. By adding a suitable partition of zero and applying Schwarz' inequality, one can construct the following upper bound:

$$\zeta = \min_{\theta \in \mathbb{R}^n} \|R(\beta_0) + \sum_{i=1}^{i=n} \theta_i r'_i\|_{\mathbb{B}} \leq \zeta' + \min_{\bar{\theta} \in \mathbb{R}^n} \|\sum_{i=1}^{i=n} \theta_i r'_i - \sum_{i=1}^{i=n} \bar{\theta}_i R'(\beta_0) \beta'_i\|_{\mathbb{B}}, \quad (4.7)$$

with $\bar{\theta}$ the argument of (4.6). If $R'(\beta_0) \text{span}\{\beta'_i\} \parallel \{r'_i\}$ then the second term in the upper bound vanishes and it follows that $\zeta = \zeta'$. However, if the principal angle between $R'(\beta_0) \text{span}\{\beta'_i\}$ and $\text{span}\{r'_i\}$ is large, then ζ can be much larger than ζ' . The essential problem is that this discrepancy can persist even if the sequences $\{\beta'_i\}$ and $\{r'_i\}$ are augmented. In fact, it is possible that

$$\text{span}\{r'_i\} \cup R'(\beta_0) \text{span}\{\beta'_i\}^\perp \subset \mathbb{B} \quad i = 1, \dots, n, \quad (4.8)$$

despite $R'(\beta_0) \mathbb{B} = \mathbb{B}$. If (4.8) holds and the search directions are orthonormalised, augmentation of the residual sensitivities yields only a subspace of \mathbb{B} . Consequently, $\zeta \not\rightarrow 0$ as n increases. This can result in a failure of the algorithm, as the residual estimate ζ need not decrease below the tolerance ϵ_1 for any n . The algorithm then stalls in the inner loop. For an example of such algorithmic failure, see Sec. 5.

Further to the aforementioned algorithmic failure, the method can fail due to poor approximation properties of the residual sensitivities $\{r'_i\}$: If $\{r'_i\}$ is too disparate from $R'(\beta_0) \text{span}\{\beta'_i\}$, then the computed optimal update $\sum \theta_k \beta'_k$ based on $\{r'_i\}$ can be counter effective and can lead to an *increase* of the residual, even if an update based on $R'(\beta_0) \text{span}\{\beta'_i\}$ would have produced an effective reduction. The method with reuse then becomes unstable. For a further elaboration of such approximation failure, we refer to Ref. [19].

with ℓ and ρ the length and density corresponding to the uniform state, respectively. Eq. (5.3) admits infinitely many ω , corresponding to the different modes of the fluid-structure system. Furthermore, Ref. [7] establishes that the convergence of the subiteration method degrades with the time-interval length τ , and that the convergence deteriorates linearly with $\rho c/\sqrt{km}$ in the absence of reflections within a time step, i.e., for $\tau \leq 2\ell/c$. If reflections within a time step occur, the scaling of the subiteration operator changes and, in particular, for fixed time-step size the convergence deteriorates linearly with $\rho c^2/k\ell$ in the limit $\ell/c \rightarrow 0$. Below, we consider several representative settings of these parameters.

The selected discretisation procedure for the piston system is essentially identical to that in [8]. The space/time domain of the fluid is covered with a tessellation of quadrilateral elements. The number of elements in the spatial direction is indicated by $N_{\mathbb{U}}^x$, the number of elements in the temporal direction per unit time by $N_{\mathbb{U}}^t$. The structure mesh comprises $N_{\mathbb{Z}}$ elements per unit time. The fluid and structure equations are discretised by means of discontinuous Galerkin methods. The approximation space for the structure consists of piecewise polynomials of degree $P_{\mathbb{Z}}$. The approximation space for the fluid consists of piecewise tensor products of polynomials of degree $P_{\mathbb{U}}$. The approximation spaces admit discontinuities across element boundaries. The elements in the fluid are connected by the modified Osher scheme and weakly enforced initial conditions. The connection between the elements in the structure is provided by weakly enforced initial conditions. The interface approximation spaces $\tilde{\mathbb{A}}$ and $\tilde{\mathbb{P}}$ comprise $N_{\mathbb{A},\mathbb{P}}$ elements per unit time, and consist of piecewise polynomials of degree $P_{\mathbb{A}}$ and $P_{\mathbb{P}}$, respectively.

5.2 Functional Setting

To appropriately analyse the results and perform the GMRES acceleration, the function spaces \mathbb{A}, \mathbb{Z} and \mathbb{P} must be specified for the model problem. Note that for the model problem the structure displacement and the structure-interface displacement are identical, i.e., $z = z|_{\Theta} \in \mathbb{Z}$. Let $\mathcal{T} :=]0, \tau[$ denote the computational time interval under consideration and let $L^2(\mathcal{T})$ be the standard space of square-integrable functions on \mathcal{T} . Furthermore, we define the Sobolev space $H^1(\mathcal{T})$ in the usual manner:

$$H^1(\mathcal{T}) := \{f : \|f\|_{H^1(\mathcal{T})} < \infty\} \quad (5.4)$$

with

$$\|\cdot\|_{H^1(\mathcal{T})}^2 := \langle \cdot, \cdot \rangle_{H^1(\mathcal{T})}, \quad \langle f, g \rangle_{H^1(\mathcal{T})} := \langle f, g \rangle_{L^2(\mathcal{T})} + \langle Df, Dg \rangle_{L^2(\mathcal{T})}, \quad (5.5)$$

where D indicates the differentiation operator. The analysis in [7] conveys that a proper functional setting is $\mathbb{A} = \mathbb{Z} = H^1(\mathcal{T})$ and $\mathbb{P} = L^2(\mathcal{T})$.

To express the inner product of a pair of functions β_0, β_1 in a finite-element-approximation space $\tilde{\mathbb{B}} \subset \mathbb{B}$ ($= H^1(\mathcal{T}), L^2(\mathcal{T})$) in terms of the coefficients $\{\check{\beta}_{0i}\}$ and $\{\check{\beta}_{1i}\}$ with respect to a basis $\{\hat{\beta}_i\}$ of $\tilde{\mathbb{B}}$, we note that

$$\langle \beta_0, \beta_1 \rangle_{\mathbb{B}} = \sum_{i=1}^{\dim \tilde{\mathbb{B}}} \sum_{j=1}^{\dim \tilde{\mathbb{B}}} \check{\beta}_{0i} W_{ij} \check{\beta}_{1j} = \check{\beta}_0^T \cdot \mathbf{W} \cdot \check{\beta}_1 \quad \text{with} \quad W_{ij} := \langle \hat{\beta}_i, \hat{\beta}_j \rangle_{\mathbb{B}}. \quad (5.6)$$

In Eq. (5.6), the coefficient vectors $\check{\beta}_i$ designate $\check{\beta}_i := (\check{\beta}_{i1}, \check{\beta}_{i2}, \dots)$. The Gram matrix \mathbf{W} is symmetric positive definite and, hence, it admits a Cholesky factorisation, i.e., there exists an upper triangular matrix \mathbf{Q} such that $\mathbf{W} = \mathbf{Q}^T \cdot \mathbf{Q}$. Accordingly, we can express the \mathbb{B} -norm of any $\beta \in \mathbb{B}$ as:

$$\|\beta\|_{\mathbb{B}}^2 = \langle \beta, \beta \rangle_{\mathbb{B}} = \check{\beta}^T \cdot \mathbf{W} \cdot \check{\beta} = \check{\beta}^T \cdot \mathbf{Q}^T \cdot \mathbf{Q} \cdot \check{\beta} = \|\mathbf{Q} \cdot \check{\beta}\|_2^2, \quad (5.7)$$

where $\|\cdot\|_2$ connotes the standard vector 2-norm. Eqs. (5.6)-(5.7) are used to compute the inner products and norms in Algorithms 1-3 and, moreover, to determine norms in the analysis of the results in the ensuing paragraphs.

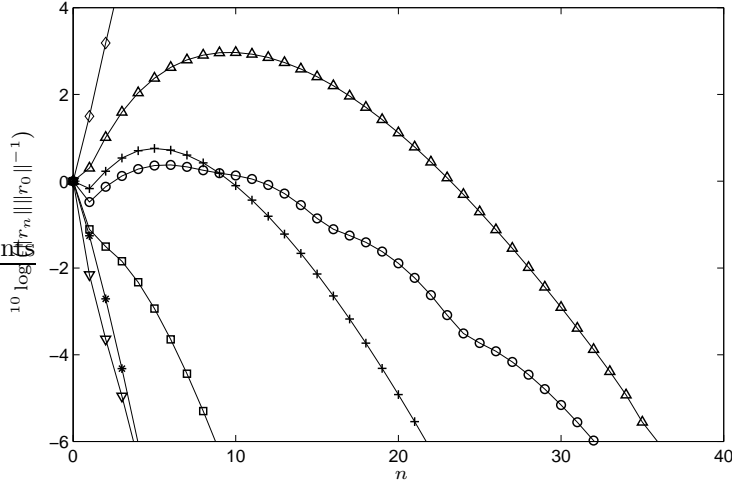


Figure 2: Convergence of the subiteration method: reduction of the displacement residual $\|r_n\|_{H^1} \|r_0\|_{H^1}^{-1}$ for $\tau = 1, \Upsilon = 0.1$ (∇), $\tau = 0.1, \Upsilon = 1$ (*), $\tau = 1, \Upsilon = 1$ (\square), $\tau = 1, \Upsilon = 5$ (+), $\tau = 10, \Upsilon = 1$ (\circ), $\tau = 1, \Upsilon = 10$ (\triangle), $\tau = 1, \Upsilon = 100$ (\diamond).

Fig.	ℓ	k	m	c	χ	ρ	τ	N_{U}^x	N_{U}^t	N_{Z}	$N_{\text{A},\text{P}}$	P_{U}	P_{Z}	P_{A}	P_{P}
2–4	1	1	1	0.2	10^{-6}	*	*	20	20	20	20	2	3	3	2
5	1	1	1	0.2	$5 \cdot 10^{-3}$	50	1	20	20	20	20	2	3	3	2
6	1	1	1	0.2	*	50	1	N	N	N	N	P	$P+1$	$P+1$	P

Table 2: System and discretisation parameters for test case 1 (Figs. 2-6). Variable parameters indicated by *.

5.3 Test Case 1

The first test case concerns the recovery of a uniform solution in a single time interval. We specify the initial conditions for the fluid as $u^0 = (\rho, 0, e)$, with ρ and e constants. The initial conditions for the structure are specified as $z^0 = \dot{z}^0 = 0$. Moreover, we set the external force to $p^0 := p(u^0) = (a-1)e$. The obvious solution to the fluid-structure-interaction problem is then $u = (\rho, 0, e)$, $z = \alpha = 0$ and $\pi = p^0$. To determine the properties of the subiteration method and of the Interface-GMRES(R)-accelerated subiteration method, we instead provide an initial approximation $z_0(t) = \chi(10t)^2 \exp(-(10t)^2 + 1)$. The initial approximation is chosen such that $z_0(0) = \dot{z}_0(0) = 0$, in accordance with the initial conditions, and $\max_{t \in [0, \infty)} z_0(t) = \chi$.

Figure 2 displays the reduction in the displacement residual $\|r_n\|_{H^1} \|r_0\|_{H^1}^{-1}$ versus the iteration counter n for the subiteration method for representative settings of the time-interval length τ and the parameter $\Upsilon := \rho c / \sqrt{km}$. The auxiliary parameters are specified in Table 2. We note that c, ρ and e are interrelated by $c = \sqrt{a(a-1)e/\rho}$. The discretisation is sufficiently accurate to ensure that the results are essentially independent of the discretisation parameters, i.e., an increase in N or P does not yield an essential change in the results. Fig. 2 illustrates that the convergence behaviour of the subiteration method deteriorates with increasing τ and Υ . For sufficiently large τ, Υ , e.g., $\tau = 1, \Upsilon = 100$, the subiteration method is unstable and $\|r_n\|_{H^1} \|r_0\|_{H^1}^{-1}$ increases indefinitely. For intermediate τ, Υ the residual increases initially before asymptotic convergence sets in. This nonmonotonous convergence behaviour is indicative of the nonnormality of the subiteration method; see Ref. [7]. Note that the initial divergence can amplify the residual by many orders of magnitude, despite formal stability. For sufficiently small τ, Υ the subiteration method converges properly.

Figure 3 displays the estimated and actual reductions in the residual $\|r_n\|_{\mathbb{B}}\|r_0\|_{\mathbb{B}}^{-1}$ for the Interface-GMRES-accelerated subiteration method with orthonormalisation for $\tau = 1$, $\Upsilon = 1, 10, 100$, and for two choices of the acceleration space \mathbb{B} and the associated inner product, viz., $(\mathbb{B}, \langle \cdot, \cdot \rangle) = (\mathbb{Z}, \langle \cdot, \cdot \rangle_{H^1})$ and $(\mathbb{B}, \langle \cdot, \cdot \rangle) = (\mathbb{P}, \langle \cdot, \cdot \rangle_{L^2})$. The tolerances in Algs. 1-2 are set relative to the initial residual according to $\epsilon_0 = 10^{-6}\|r_0\|_{\mathbb{B}}$ and $\epsilon_1 = 10^{-7}\|r_0\|_{\mathbb{B}}$. Furthermore, the norm of the updates, ν , is set relative to the initial residual as $\nu = 10^{-2}\|r_0\|_{\mathbb{B}}$. The factor 10^{-2} is in principle arbitrary. However, if $\|r_0\|_{\mathbb{B}}$ is large, e.g., as a result of largeness of Υ or τ , then a small factor can be imperative to maintain robustness of the underlying subiteration process. The auxiliary parameters are listed in Table 2. Fig. 3 illustrates that the convergence of the Interface-GMRES-accelerated subiteration method improves with decreasing Υ . Similar behaviour can be observed with decreasing τ (results not displayed). On account of the definition of the Krylov space \mathcal{K}_n and the optimality of the GMRES approximation in \mathcal{K}_n , the residual of the subiteration method separately provides an upper bound for the estimated residual, i.e., the residual of the inner Krylov process in the Interface-GMRES-accelerated method. Hence, fast convergence of the subiteration method implies fast convergence of the inner Krylov process. Generally, this translates in fast convergence of the overall accelerated method unless the linearisation error, i.e., the discrepancy between the estimated (linear) residual and the actual (nonlinear) residual, is large. This linearisation error is manifested by the jumps in the graphs in Fig. 3 at each Newton update. Because the norm of the Newton updates decreases as the process progresses, the linearisation error decreases and, accordingly, the jumps diminish. Despite this diminution, an initially large linearisation error can render the Interface-GMRES-accelerated method less efficient than the subiteration method separately. Indeed, a comparison of Figs. 2 and 3 conveys that for $\tau = 1, \Upsilon = 1$ the subiteration method separately is slightly more effective. This effect is more conspicuous if the error amplitude χ is large, because the linearisation error in the Interface-GMRES method is then more pronounced. In advance of the results in Fig. 5, however, we mention that this adverse effect of the linearisation error can be avoided straightforwardly by setting the tolerance ϵ_1 relative to the *active* nonlinear residual according to $\epsilon_1 = v\|r_j\|_{\mathbb{B}}$, with $v < 1$ a suitable positive constant. For large Υ the accelerated method is much more efficient. In fact, for $\tau = 1, \Upsilon = 100$ the subiteration method separately is unstable (see Fig. 2), while the Interface-GMRES-accelerated method with orthonormalisation is convergent. In addition, Fig. 3 conveys that the convergence properties of the Interface-GMRES-accelerated subiteration method depend only moderately on the choice of the acceleration space. Before the first Newton update the estimated residuals corresponding to the two different acceleration spaces virtually coincide, and the dependence is primarily attested by the distinct differences between the estimated residual and the actual residual. However, the differences are minute and do not seem to warrant a preference for one acceleration space to the other.

Figure 4 illustrates the implications of the choice of the acceleration space for the condition number of the least-squares minimisation problem in the Interface-GMRES-acceleration method with orthonormalisation. The figure plots $\text{cond}(\mathbf{Q} \cdot \mathbf{R}'_n)$ with $\mathbf{R}'_n := (\mathbf{r}'_1, \dots, \mathbf{r}'_n)$ versus the dimension of the acceleration space n for $(\mathbb{B}, \langle \cdot, \cdot \rangle) = (\mathbb{Z}, \langle \cdot, \cdot \rangle_{H^1})$ and $(\mathbb{B}, \langle \cdot, \cdot \rangle) = (\mathbb{P}, \langle \cdot, \cdot \rangle_{L^2})$, and for $\Upsilon = 1, 10, 100$. For reference, Fig. 4 also displays the condition numbers without orthonormalisation for $\Upsilon = 1$. Note that the maximum dimensions of the acceleration spaces associated with \mathbb{P} and \mathbb{Z} are $N_{\mathbb{P}}(P_{\mathbb{P}} + 1) = 60$ and $N_{\mathbb{Z}}(P_{\mathbb{Z}} + 1) = 80$, respectively. From Fig. 4 it can be observed that the condition numbers generally increase with increasing Υ . A similar observation pertains to the dependence on τ (results not displayed). Initially, the condition numbers corresponding to the two acceleration spaces are virtually identical. However, for $(\mathbb{Z}, \langle \cdot, \cdot \rangle_{H^1})$ the condition number increases intermittently as the dimension n increases, whereas for $(\mathbb{P}, \langle \cdot, \cdot \rangle_{L^2})$ the condition number remains essentially constant after the initial increase. Experiments with different parameter settings indicate that this property of $(\mathbb{P}, \langle \cdot, \cdot \rangle_{L^2})$ is universal for the model problem. As the accuracy of the solution to a least-squares problem deteriorates quadratically with the condition number of the system (see Ref. [12, §5.3.7-8]), $(\mathbb{P}, \langle \cdot, \cdot \rangle_{L^2})$ is preferable to $(\mathbb{Z}, \langle \cdot, \cdot \rangle_{H^1})$. However, for small to moderate n the difference is minute. Without orthonormalisation the condition number of the least-squares problem and, accordingly, the relative error in the least-squares solution exhibit fast exponential growth with increasing dimension n . This renders a method without orthonormalisation inviable.

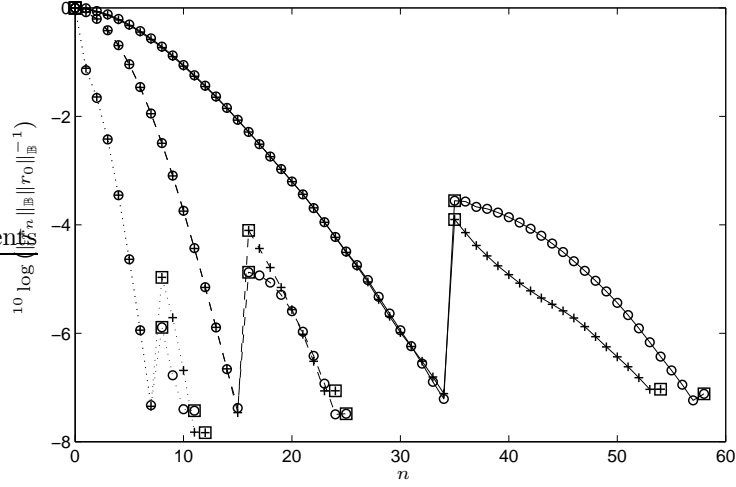


Figure 3: Convergence of the Interface-GMRES-accelerated subiteration method with orthonormalisation: estimated and actual residual reduction $\|r_n\|_{\mathbb{B}} \|r_0\|_{\mathbb{B}}^{-1}$ for $\tau = 1$, $\Upsilon = 1$ (\cdots), 10 ($-\cdots$), 100 ($—$) and $(\mathbb{B}, \langle \cdot, \cdot \rangle) = (\mathbb{Z}, \langle \cdot, \cdot \rangle_{H^1})$ (+), $(\mathbb{B}, \langle \cdot, \cdot \rangle) = (\mathbb{P}, \langle \cdot, \cdot \rangle_{L^2})$ (\circ). Symbols indicate estimated residuals. Newton updates (actual residuals) marked by \square .

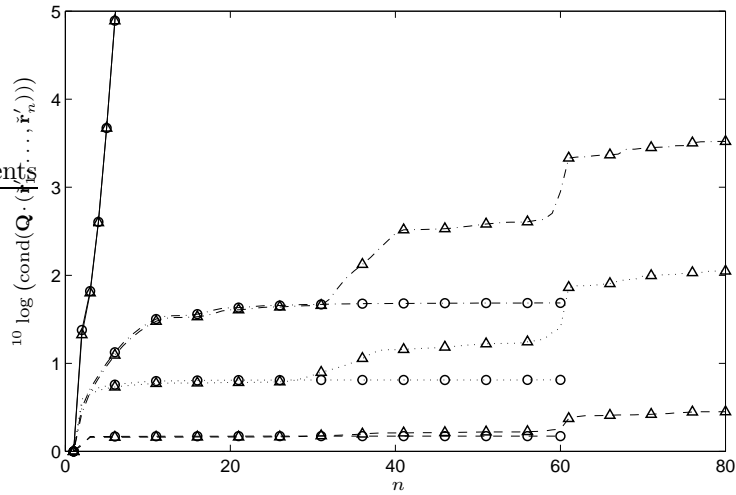


Figure 4: Condition number of the least-squares minimisation problem in the Krylov process for $(\mathbb{B}, \langle \cdot, \cdot \rangle) = (\mathbb{Z}, \langle \cdot, \cdot \rangle_{H^1})$ (\triangle) and $(\mathbb{B}, \langle \cdot, \cdot \rangle) = (\mathbb{P}, \langle \cdot, \cdot \rangle_{L^2})$ (\circ), and for $\Upsilon = 1$ ($-\cdots$), 10 (\cdots), 100 ($—$). Condition number without orthonormalisation for $\Upsilon = 1$ ($—$).

Next, we consider the effects of a relative tolerance on the estimated residuals, conforming to $\epsilon_1 = v \|r_j\|_{\mathbb{B}}$ ($0 < v < 1$), and exertion of the reuse option within the Newton process. The relative tolerance serves to avoid the computational squandering incurred by excessively accurate solution of the linear problems: if the linearisation error is large, then a strict reduction of the linear residual does not yield an according reduction of the nonlinear residual anyway. Figure 5 plots the residual reduction $\|r_n\|_{\mathbb{B}} \|r_0\|_{\mathbb{B}}^{-1}$ for $(\mathbb{B}, \langle \cdot, \cdot \rangle) = (\mathbb{Z}, \langle \cdot, \cdot \rangle_{H^1})$, $\chi = 5 \cdot 10^{-3}$, $\tau = 1$, $\Upsilon = 10$ and $v = 10^{-4}, 10^{-1}$. Other parameters are listed in Table 2. It is to be noted that the nonlinearity pertaining to the current setting is stronger than before on account of $\chi = 5 \cdot 10^{-3}$ instead of $\chi = 10^{-6}$. For transparency, results for $(\mathbb{B}, \langle \cdot, \cdot \rangle) = (\mathbb{P}, \langle \cdot, \cdot \rangle_{L^2})$ are not displayed in Fig. 5. However, these results are very similar, and the following discussion applies to them likewise. Regarding the results without reuse in Fig. 5, one can observe that for a relative tolerance of $v = 10^{-1}$ the discrepancy between the estimated residual and the actual residual is notable only in the first Newton step, whereas for $v = 10^{-4}$ there is a significant discrepancy at each update. Hence, for $v = 10^{-4}$ the linear system is solved excessively accurate, resulting in higher overall computational cost. A comparison of the result for $v = 10^{-1}$ with reuse to the results for $\Upsilon = 10$, $(\mathbb{B}, \langle \cdot, \cdot \rangle) = (\mathbb{Z}, \langle \cdot, \cdot \rangle_{H^1})$ in Fig. 3 conveys that with the reuse option the convergence of the *nonlinear* residual (Fig. 5) is similar to the convergence of the estimated *linear* residual (Fig. 3), except for the intermediate Newton updates. Indeed, the left plot in Fig. 5 shows that with the reuse option a reduction of the nonlinear residual $\|r_n\|_{\mathbb{B}} \|r_0\|_{\mathbb{B}}^{-1} \leq 10^{-6}$ is obtained in 22 subiterations, of which 7 are spent on updates of the nonlinear residual, while in Fig. 3 the estimated residual converges to $\|r_n\|_{\mathbb{B}} \|r_0\|_{\mathbb{B}}^{-1} \leq 10^{-6}$ in 14 subiterations. As such, the reuse option in combination with a relative tolerance mitigates the effect of nonlinearity. However, the right plot in Fig. 5 illustrates that the efficiency improvement offered by the reuse option is at the expense of robustness: with reuse and a relative tolerance of $v = 10^{-4}$ the linear residual estimate stalls, and the method malfunctions. In accordance with the theory in §4.3, the stall of the estimated residual is preceded by a substantial rotation of the image of the search directions under the active residual derivative compared to the available residual sensitivities. In Fig. 5 this rotation is evidenced by the fact that the first Newton update yields a decrease in the actual nonlinear residual (difference between A and B in Fig. 5), but an increase in the estimated residual (difference between C and D). It is to be noted that for $v = 10^{-1}$, on the other hand, the increases in the residual estimates over the Newton iterations are negligible. We remark that the disparity between the estimated residuals before and after the Newton update in relation to the difference between the actual nonlinear residuals before and after the Newton update can serve as a basis for a feasibility indicator for the reuse option.

Finally, we verify the asymptotic mesh independence of the convergence behaviour of the subiteration method with and without Interface-GMRES(R) acceleration. To this end, we reconsider the test case with $\tau = 1$, $\Upsilon = 10$ on meshes with different mesh widths and different orders of approximation. In particular, we choose the approximation spaces such that $N_{\mathbb{U}}^x = N_{\mathbb{U}}^t = N_{\mathbb{Z}} = N_{\mathbb{A}, \mathbb{P}} =: N$ with $N = 5, 10, 20$, $P_{\mathbb{U}} = P_{\mathbb{P}} =: P$ and $P_{\mathbb{Z}} = P_{\mathbb{A}} = P + 1$ with $P = 2, 4, 6$. The results are displayed in Fig. 6. The plots in Fig. 6 indeed indicate that the convergence behaviour of the subiteration method and of the Interface-GMRES(R)-accelerated subiteration method is asymptotically independent of the mesh width and order of the approximation spaces, i.e., for all sufficiently fine meshes or sufficiently high orders of the polynomial approximation the convergence plots coincide. Let us remark that we have tacitly assumed that the intermediate iterates are sufficiently regular for p -refinement to yield fast convergence; see, e.g., Ref. [20, Th.6.8].

5.4 Test Case 2

The second test case serves to test the Interface-GMRESR method with reuse of the Krylov space in consecutive time steps. The fluid and structure are provided with initial conditions corresponding to a superposition of the primary and secondary periodic mode of the linearised system; cf. Ref. [8]. In particular, the initial conditions on the fluid density (u_1) and momentum (u_2), and the structure

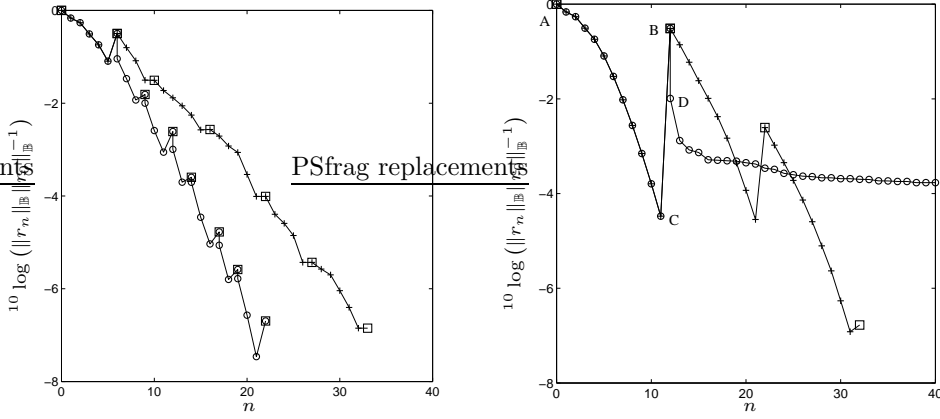


Figure 5: Convergence of the Interface-GMRESR-accelerated subiteration method with (\circ) and without $(+)$ reuse: estimated and actual residual reduction $\|r_n\|_{\mathbb{B}}\|r_0\|_{\mathbb{B}}^{-1}$ for $\chi = 5 \cdot 10^{-3}$, $\tau = 1$, $\Upsilon = 10$, and $(\mathbb{B}, \langle \cdot, \cdot \rangle) = (\mathbb{Z}, \langle \cdot, \cdot \rangle_{H^1})$, for $\nu = 10^{-1}$ (left) and $\nu = 10^{-4}$ (right). Symbols indicate linear residuals. Nonlinear residuals marked by \square . See text for connotation A,B,C,D.

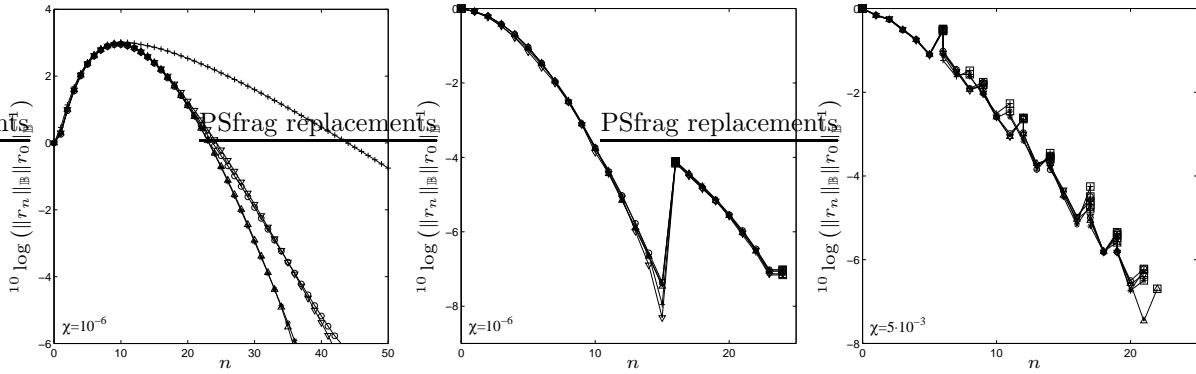


Figure 6: Mesh dependence: convergence of the subiteration method (left), with GMRES acceleration (center), and GMRESR acceleration (right), for $\tau = 1$, $\Upsilon = 10$, and $N = 5, P = 2$ ($+$), $N = 10, P = 2$ (\circ), $N = 20, P = 2$ (\triangle), $N = 5, P = 4$ (∇), and $N = 5, P = 6$ ($*$). Symbols indicate linear residuals. Nonlinear residuals marked by \square .

case	ℓ	k	m	c	χ	ρ	ω_0	ω_1	τ	$N_{\mathbb{U}}^x$	$N_{\mathbb{U}}^t$	$N_{\mathbb{Z}}$	$N_{\mathbb{A},\mathbb{P}}$	$P_{\mathbb{U}}$	$P_{\mathbb{Z}}$	$P_{\mathbb{A}}$	$P_{\mathbb{P}}$
a	1	1	1	0.2	0.1	50	0.36	0.95	10	20	20	10	10	2	9	9	8
b	1	1	1	5	0.05	1	4.39	1.71	1	40	40	10	10	2	9	9	8
c	1	1	1	1	0.1	1	1.21	3.45	1	20	20	10	10	2	9	9	8

Table 3: System and discretisation parameters for test case 2 (Figs. 7-9), and corresponding primary and secondary radian frequencies ω_0 and ω_1 conforming to (5.3). $N_{\mathbb{U}}^t$ denotes the number of fluid elements in temporal direction per time step.

displacement and velocity, are determined from the initial values of:

$$\begin{pmatrix} u_1 \\ u_2 \end{pmatrix} = \begin{pmatrix} \rho \\ 0 \end{pmatrix} - \chi \sum_{i=0}^{i=1} 10^{-i} \frac{\rho \ell \omega_i}{c \sin(\omega_i \ell / c)} \begin{pmatrix} \cos(\omega_i x / c) \cos(\omega_i t) \\ c \sin(\omega_i x / c) \sin(\omega_i t) \end{pmatrix}, \quad z = \chi \sum_{i=0}^{i=1} 10^{-i} \ell \cos(\omega_i t). \quad (5.8)$$

The initial conditions on the fluid energy (u_3) are determined from the isentropy condition. The radian frequencies ω_0, ω_1 of the primary and secondary mode are subject to (5.3). The ratio 10^{-1} of the amplitudes of the secondary and the primary mode has been selected arbitrarily. To test the capabilities of the GMRESR method under adverse conditions, we select a strongly nonlinear setting. Three different settings of the experiment are considered; see Table 3. It is to be noted that, at variance with Tab. 2, $N_{\mathbb{U}}^t$ in Tab. 3 designates the number of elements in the temporal direction per time step. The first setting is characterised by a high density, a large computational time step, and the absence of reflections in the fluid within a computational time step, i.e., $\tau \leq 2\ell/c$. The subiteration method is unstable for this setting; cf. Ref. [7]. The second setting concerns a case with reflections within a computational time step, i.e., $\tau > 2\ell/c$. The subiteration method is formally stable for this setting, but fails due to the initial nonnormality-induced divergence. The final setting is chosen such that the subiteration method converges properly. This setting serves to compare the capabilities of the subiteration method and of the Interface-GMRESR-accelerated method under favourable conditions for the subiteration method. For all computations the tolerance ϵ_0 is set relative to the initial residual according to $\epsilon_0 = 10^{-3} \|r_0\|_{\mathbb{B}}$, i.e., within each time step a residual reduction of 10^{-3} is required. Moreover, the tolerance ϵ_1 in the Interface-GMRESR method is set relative to the *active* nonlinear residual as $\epsilon_1 = \nu \|r_j\|_{\mathbb{B}}$ with $\nu = 10^{-1/2}$, and the underrelaxation parameter ν is set relative to the initial residual in the first time step according to $\nu = 10^{-3} \|r_0\|_{\mathbb{B}}$.

Figure 7 displays the residual reduction versus the number of subiterations in the first and tenth time step for test cases 2^{a-c} for the subiteration method separately, and for the Interface-GMRESR-accelerated method with $(\mathbb{B}, \langle \cdot, \cdot \rangle) = (\mathbb{Z}, \langle \cdot, \cdot \rangle_{H^1}), (\mathbb{P}, \langle \cdot, \cdot \rangle_{L^2})$. Notice the different scalings of the top and bottom figures. We remark that for test cases 2^{a,b} the aforementioned divergence of the subiteration method prohibits the evaluation of the residual after a single iteration. In contrast, for test case 2^a the Interface-GMRESR-accelerated method functions properly for both choices of the acceleration space, despite the instability of the underlying subiteration method. In the first time step (Fig. 7, top left), most iterations are expended on the construction of the Krylov space. However, by virtue of the reuse of the Krylov space, increasingly few iterations are required for this purpose in subsequent time steps (Fig. 7, bottom left). Eventually, all iterations are spent on the evaluation of the nonlinear residuals, except for occasional augmentations of the Krylov space. It is notable that $(\mathbb{Z}, \langle \cdot, \cdot \rangle_{H^1})$ yields a more effective acceleration than $(\mathbb{P}, \langle \cdot, \cdot \rangle_{L^2})$; see also Fig. 8. For test case 2^b (Fig. 7 center) the properties of the Interface-GMRESR-acceleration method depend pivotally on the acceleration space: Whereas the method with $(\mathbb{Z}, \langle \cdot, \cdot \rangle_{H^1})$ functions properly, the method with $(\mathbb{P}, \langle \cdot, \cdot \rangle_{L^2})$ fails in the first time step. To elaborate this difference, let us note that for $(\mathbb{Z}, \langle \cdot, \cdot \rangle_{H^1})$ the mapping $\Lambda : z_{j-1} \mapsto z_j$ ($\Lambda : \pi_{j-1} \mapsto \pi_j$ for $(\mathbb{P}, \langle \cdot, \cdot \rangle_{L^2})$) induced by the subiteration method can be decomposed as $\Lambda = \Lambda_1 \Lambda_0$ (respectively $\Lambda_0 \Lambda_1$) with $\Lambda_0 : z_{j-1} \mapsto \pi_j$ and $\Lambda_1 : \pi_j \mapsto z_j$. Because the nonlinearity of the composite operators $\Lambda_1 \Lambda_0$ and $\Lambda_0 \Lambda_1$ can be very different and, moreover, the GMRES(R)-acceleration method is based on linear approximation, for strongly nonlinear problems

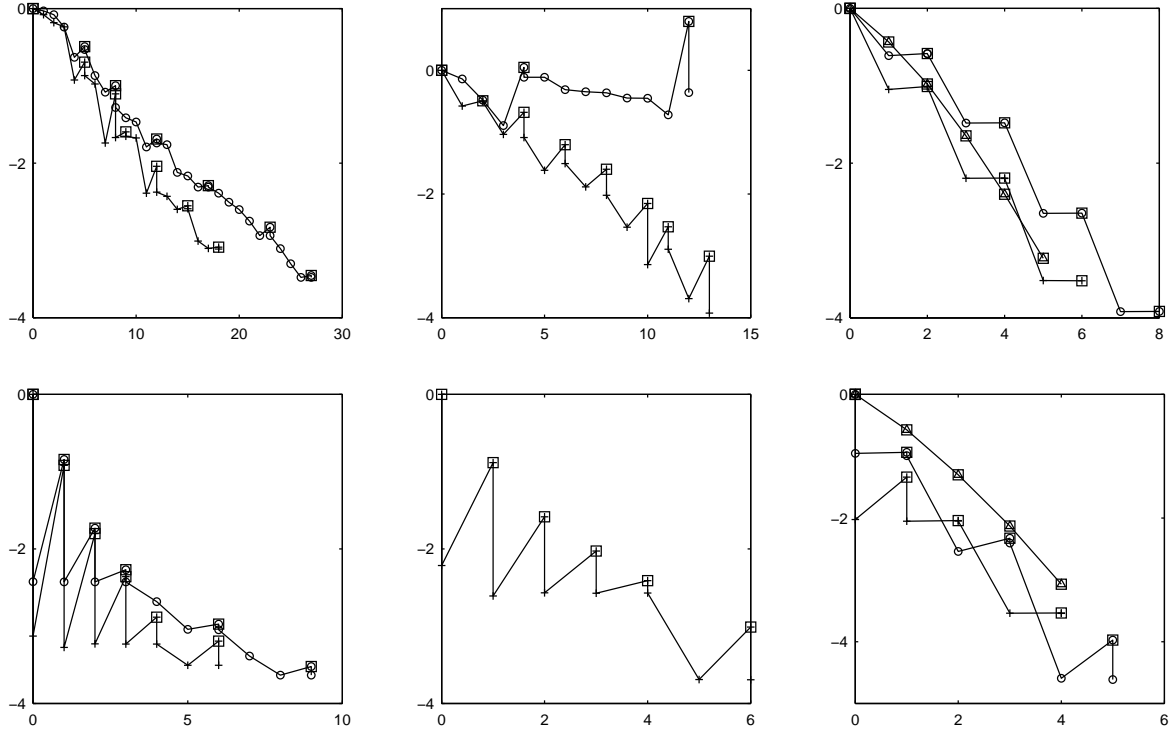


Figure 7: Residual reduction $\|r_n\|_{\mathbb{B}}\|r_0\|_{\mathbb{B}}^{-1}$ versus number of iterations for test case 2^a (left), 2^b (center), and 2^c (right) in time step 1 (top) and time step 10 (bottom) for the subiteration method (\triangle), and the Interface-GMRESR-accelerated method with $(\mathbb{B}, \langle \cdot, \cdot \rangle) = (\mathbb{P}, \langle \cdot, \cdot \rangle_{L^2})$ (\circ) and $(\mathbb{Z}, \langle \cdot, \cdot \rangle_{H^1})$ ($+$). Symbols $\circ, +$ indicate estimated residuals. Actual residuals marked by \square .

$(\mathbb{Z}, \langle \cdot, \cdot \rangle_{H^1})$ and $(\mathbb{P}, \langle \cdot, \cdot \rangle_{L^2})$ can yield profoundly different convergence behaviour. Finally, the results of test case 2^c in Fig. 7 (right) illustrate that even under favourable conditions for the subiteration method, the effectiveness of the GMRESR-accelerated method is still similar; see also Fig. 8.

Figure 8 plots the cumulative number of iterations and the dimension of the Krylov space versus the time step counter for test cases 2^{a-c} . The figure shows that the construction of an appropriate Krylov subspace requires relatively many iterations in the first few time steps, and the computational expenditure is correspondingly high. However, once a suitable subspace has been obtained, only occasional augmentations of this subspace are required. The computational cost per time step is then determined by the growth rate of the Krylov space and the number of nonlinear-residual evaluations within each time step. Fig. 8 exhibits that in general the growth rate pertaining to $(\mathbb{Z}, \langle \cdot, \cdot \rangle_{H^1})$ is much lower than that for $(\mathbb{P}, \langle \cdot, \cdot \rangle_{L^2})$. However, because the computational cost is dominated by the nonlinear-residual evaluations, the effect on the computational expenditure is small. The results for test case 2^c show that under conditions that are favourable for the subiteration method and adverse for the Interface-GMRESR-accelerated method, the computational cost of the Interface-GMRESR-accelerated method is still very similar to that of the subiteration method separately. In fact, the accelerated method with $(\mathbb{Z}, \langle \cdot, \cdot \rangle_{H^1})$ is even slightly more effective. Moreover, it is noteworthy that the acceleration method with $(\mathbb{Z}, \langle \cdot, \cdot \rangle_{H^1})$ yields an average computational expenditure of less than 10 iterations per time step for test case 2^a . In contrast, Fig. 3 conveys that the subiteration method requires 30 iterations to achieve a reduction of the residual of 10^{-3} for the same setting of c, Υ and a 10 times smaller time step.

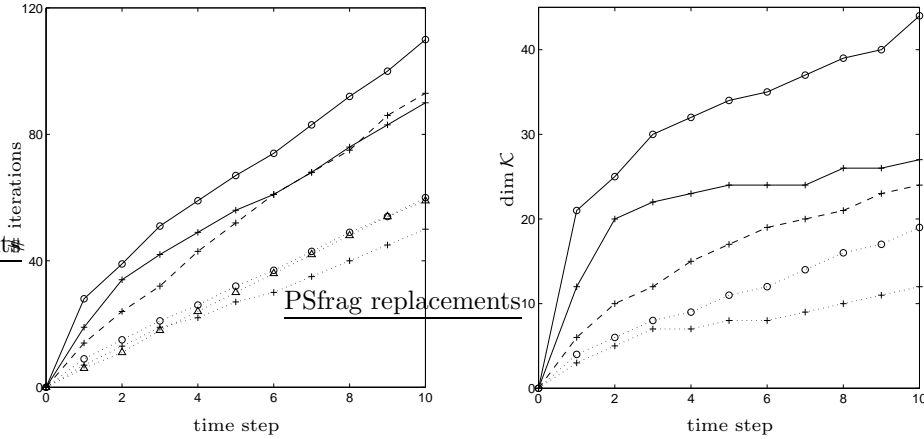


Figure 8: Cumulative number of iterations (*left*) and dimension of Krylov space (*right*) for test case 2^a (—), 2^b (---) and 2^c (···) for subiteration (\triangle) and the Interface-GMRESR method with $(\mathbb{B}, \langle \cdot, \cdot \rangle) = (\mathbb{P}, \langle \cdot, \cdot \rangle_{L^2})$ (\circ) and $(\mathbb{Z}, \langle \cdot, \cdot \rangle_{H^1})$ ($+$).

Finally, Figure 9 displays the space-time domain occupied by the fluid, and the density in the fluid for test cases 2^{a-c} . The figure shows that the interface sustains a significant displacement, with according density fluctuations in the fluid. Moreover, the reflection of the sharp waves induced by the secondary mode are clearly visible. Considering the significant differences in the solution of the fluid-structure interaction problem between the time steps, the effectivity of the reuse option is remarkable.

6. Conclusion

We investigated GMRES(R) acceleration of the basic subiteration method for solving the aggregated equations in fluid-structure-interaction problems. We showed that the subiteration method can essentially be condensed into a fixed-point iteration for functions on the interface. Accordingly, the Krylov space in the GMRES(R) method only needs to contain vectors in a low-dimensional subspace associated with the discrete representation of such interface functions. The corresponding Interface-GMRES(R)-acceleration method requires only negligible computational resources, and retains the modularity of the underlying subiteration method and its avoidance of shape derivatives. Moreover, the Krylov space can be optionally reused in subsequent invocations of the GMRES method. The convergence behaviour of the Interface-GMRES(R)-accelerated subiteration method was inferred to be asymptotically mesh independent.

Numerical results for a prototypical model problem were presented. The results illustrate that the efficiency of the Interface-GMRES-accelerated subiteration method depends on the convergence behaviour of the underlying subiteration method and on the nonlinearity of the problem. However, the accelerated method generally attains convergence even if the subiteration method separately is unstable. Moreover, the use of a suitable relative tolerance in the inner loop of the acceleration method and in combination with the reuse option renders the dependences weak. The numerical results convey that the reuse option generally offers a substantial improvement in the efficiency of the acceleration method, but must be exercised with some caution as it can cause the acceleration method to malfunction. With a suitable choice of the relative tolerance, however, the reuse option functioned properly for all considered test cases. In general, after the initial construction of a suitable Krylov subspace only occasional augmentations of the space occur. The reuse of the Krylov space in successive time steps enables the solution of the aggregated fluid-structure equations in a few iterations per time step.

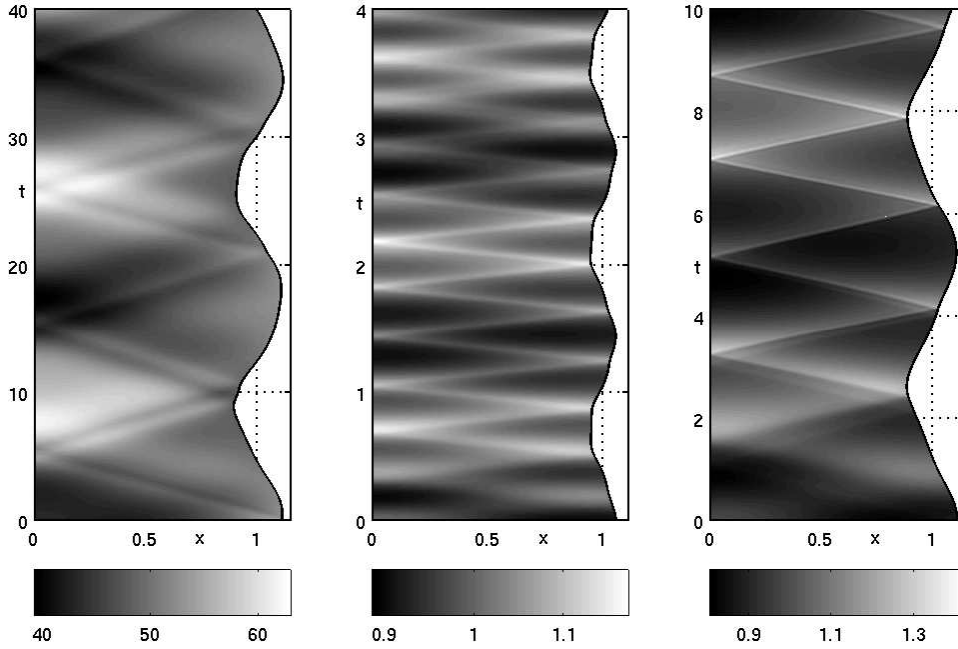


Figure 9: Space-time fluid domain and density (colour bars) for test case 2^a (left), 2^b (center), 2^c (right).

Two different interface acceleration spaces were considered, viz., the interface-pressure and the interface-displacement space. For the considered test cases, the condition numbers of the least-squares minimisation problems in the acceleration method remain within useful bounds for both acceleration spaces. Typically, displacement acceleration is slightly more effective than pressure acceleration. However, the convergence properties pertaining to the two acceleration spaces can be very different on account of differences in the nonlinearity of the associated fixed-point operators. For a strongly nonlinear test case, we observed that displacement acceleration functions properly, whereas pressure acceleration fails. The numerical results warrant a preference for displacement acceleration over pressure acceleration for the considered model problem.

Numerical experiments with different approximation spaces confirm that the convergence behaviour of the Interface-GMRES(R)-accelerated subiteration method is asymptotically independent of the mesh width and the order of the discrete approximation space.

In general, the Interface-GMRES(R) acceleration provides a substantial improvement in the robustness and efficiency of the subiteration method. Under conditions that are favourable for the conventional subiteration method and adverse for the Interface-GMRES(R)-accelerated method, the accelerated method is still more efficient. Typically, the Interface-GMRESR method with reuse of the Krylov space in successive time steps enables the solution of the aggregated equations to sufficient accuracy in a few iterations per time step, even if the subiteration method separately requires tenfolds more or fails due to instability or nonnormality-induced divergence. Moreover, the method is generic and its implementation in existing codes based on the conventional subiteration method is straightforward, although the specific properties of the method generally depend on the fluid-structure-interaction problem under consideration.

References

- [1] J.J. ALONSO AND A. JAMESON, *Fully-implicit time-marching aeroelastic solutions*, AIAA **0056** (1994), 1–13.
- [2] M. BATHE AND R.D. KAMM, *A fluid-structure interaction finite element analysis of pulsatile blood flow through a compliant stenotic artery*, Journal of Biomechanical Engineering **121** (1999), 361–369.
- [3] K. BÖHMER, P.W. HEMKER, AND H.J. STETTER, *The defect correction approach*, Computing **5** (1984), 1–32.
- [4] S.C. BRENNER AND L.R. SCOTT, *The mathematical theory of finite element methods*, 2nd ed., Texts in Applied Mathematics, vol. 15, Springer, Berlin, 2002.
- [5] L.L. BRODERICK AND J.W. LEONARD, *Nonlinear response of membranes to ocean waves using boundary and finite elements*, Ocean Engng. **22** (1995), 731–745.
- [6] P.N. BROWN AND Y. SAAD, *Hybrid Krylov methods for nonlinear systems of equations*, SIAM J. Sci. Stat. Comput. **11** (1990), 450–481.
- [7] E.H. VAN BRUMMELEN AND R. DE BORST, *On the nonnormality of subiteration for a fluid-structure interaction problem*, SIAM J. Sci. Comput. (2004), (Accepted for publication). Preprint available at <http://www.em.lr.tudelft.nl/~brummelen/publications/NonNorm2003.pdf>.
- [8] E.H. VAN BRUMMELEN, S.J. HULSHOFF, AND R. DE BORST, *Energy conservation under incompatibility for fluid-structure interaction problems*, Comput. Methods Appl. Mech. Engrg. **192** (2003), 2727–2748.
- [9] C. FARHAT, P. GEUZAIN, AND G. BROWN, *Application of a three-field nonlinear fluidstructure formulation to the prediction of the aeroelastic parameters of an f-16 fighter*, Computers and Fluids **32** (2003), 3–29.
- [10] C. FARHAT, P. GEUZAIN, AND C. GRANDMONT, *The discrete geometric conservation law and the nonlinear stability of ALE schemes for the solution of flow problems on moving grids*, J. Comput. Phys. **174** (2001), 669–694.
- [11] C.A. FELIPPA, K.C. PARK, AND C. FARHAT, *Partitioned analysis of coupled mechanical systems*, Comput. Methods Appl. Mech. Engrg. **190** (2001), 3247–3270.
- [12] G.H. GOLUB AND C.F. VAN LOAN, *Matrix computations*, Johns Hopkins, 1996.
- [13] A. GREENBAUM, *Iterative methods for solving linear systems*, Frontiers in Applied Mathematics, vol. 17, SIAM, Philadelphia, 1997.
- [14] M. HEIL, *Stokes flow in an elastic tube – a large-displacement fluid-structure interaction problem*, Int. J. Num. Meth. Fluids **28** (1998), 243–265.
- [15] M. HEIL, *An efficient solver for the fully-coupled solution of large-displacement fluid-structure interaction problems*, Comput. Methods Appl. Mech. Engrg. **193** (2004), 1–23.
- [16] P. LETALLEC AND J. MOURO, *Fluid structure interaction with large structural displacements*, Comput. Methods Appl. Mech. Engrg. **190** (2001), 3039–3067.
- [17] H.G. MATTHIES AND J. STEINDORF, *Partitioned strong coupling algorithms for fluid-structure interaction*, Comput. Struct. **81** (2003), 805–812.

- [18] R.B. MELVILLE AND S.A. MORTON, *Fully-implicit aeroelasticity on overset grid systems*, AIAA **98-0521** (1998).
- [19] C. MICHLER, E.H. VAN BRUMMELEN, AND R. DE BORST, *Error-amplification analysis of subiteration-preconditioned GMRES for fluid-structure interaction*, Comput. Methods Appl. Mech. Engrg. (2004), (Submitted for publication).
- [20] J.T. ODEN AND J.N. REDDY, *An introduction to the mathematical theory of finite elements*, Pure and Applied Mathematics, John Wiley & Sons, New York, 1974.
- [21] S. PIPERNO, C. FARHAT, AND B. LARROUTUROU, *Partitioned procedures for the transient solution of coupled aeroelastic problems – part I: Model problem, theory and two-dimensional application*, Comput. Methods Appl. Mech. Engrg. **124** (1995), 79–112.
- [22] O. PIRONNEAU, *Optimal shape design for elliptic systems*, Computational Physics, Springer, Berlin, 1984.
- [23] S.M. RIFAI ET AL., *Multiphysics simulation of flow-induced vibrations and aeroelasticity on parallel computing platforms*, Comput. Methods Appl. Mech. Engrg. **174** (1999), 393–417.
- [24] I. ROBERTSON, S.J. SHERWIN, AND P.W. BEARMAN, *Flutter instability prediction techniques for bridge deck sections*, Int. J. Num. Meth. Fluids **43** (2003), 1239–1256.
- [25] Y. SAAD AND M.H. SCHULTZ, *GMRES: A generalized minimal residual algorithm for solving nonsymmetric linear systems*, SIAM J. Sci. Stat. Comput. **7** (1986), 856–869.
- [26] H. SAITO AND L.E. SCRIVEN, *Study of coating flow by the finite element method*, J. Comput. Phys. **42** (1981), 53–76.
- [27] H.A. VAN DER VORST AND C. VUIK, *GMRESR: a family of nested GMRES methods*, Num. Lin. Alg. Appl. **1** (1994), 369–386.
- [28] M.E. VERBEEK, *Repairing near-singularity for dense EMC problems by adaptive basis techniques*, Num. Lin. Alg. Appl. **7** (2000), no. 617–634.
- [29] T. WASHIO AND C.W. OOSTERLEE, *Krylov subspace acceleration for nonlinear multigrid schemes*, Electronic Transactions on Numerical Analysis **6** (1997), 271–290.